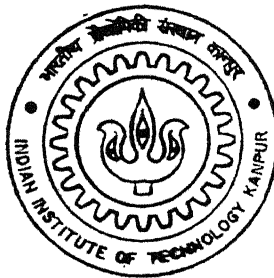


# ON APPLICATION OF MAXIMUM LIKELIHOOD METHOD AND KALMAN-FILTER TECHNIQUE TO ESTIMATE PARAMETERS FROM FLIGHT DATA OF ROCKETS AND SHELLS

By

**K. Venkat Chandra Sekhar**



Th  
AE/2004/10  
C 3610

DEPARTMENT OF AEROSPACE ENGINEERING

**Indian Institute of Technology Kanpur**

JUNE, 2004

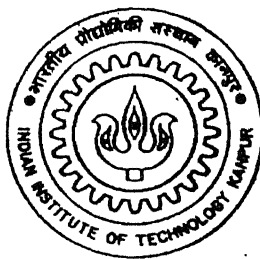
# **ON APPLICATION OF MAXIMUM LIKELIHOOD METHOD AND KALMAN-FILTER TECHNIQUE TO ESTIMATE PARAMETERS FROM FLIGHT DATA OF ROCKETS AND SHELLS**

A Thesis Submitted  
in Partial Fulfillment of the Requirements  
for the Degree of

**Master of Technology**

*by*

**K. Venkat Chandra Sekhar**



*to the*

Department of Aerospace Engineering  
**Indian Institute of Technology, Kanpur**

June 2004

28 JUL 2004/AE

इमलीसम काशीनाथ केसकर पुस्तकालय  
भारतीय प्रौद्योगिकी संस्थान कानपुर  
श्रवणिक ड० A-148451

TH

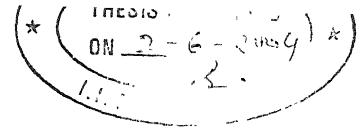
AE/2004/M

C3610



A148451

# CERTIFICATE



It is certified that the work contained in this thesis entitled, "**On application of Maximum Likelihood method and Kalman-Filter technique to estimate parameters from flight data of rockets and shells**" by K. Venkat Chandra Sekhar been carried out under my supervision and that this work has not been submitted elsewhere for a degree.

Dr. A. K. Ghosh  
Associate Professor

Department of Aerospace Engineering,  
Indian Institute of Technology,  
Kanpur – 208016.

June 2004.

## ABSTRACT

An attempt is made to estimate aerodynamic parameters using radar tracked coordinates of a free flight artillery shell. The present thesis investigates applicability of EKF and ML method to estimate aerodynamic parameters using flight data with limited information content. Due to non-availability of flight data, simulated flight data using Point Mass and Six-degree of freedom model have been generated.

In particular, study was conducted to investigate the applicability of these methods in extracting aerodynamic parameters by processing Radar tracked data obtained through different class of flight vehicle/store. These methods have been applied to flight data starting from a one-dimensional ballistic target to, an artillery shell, longitudinal motion of Short Range Strategic Missile (SM) and also to flight data of an aircraft.

The applicability of the existing methods (ML and EKF) is tested for these three different classes of flight data. It is observed that both ML and EKF can be advantageously applied to estimate few aerodynamic parameters with acceptable level of accuracy.

## ACKNOWLEDGEMENTS

With a profound sense of gratitude, I express my sincere thanks to my esteemed thesis supervisor Dr. A. K. Ghosh for his invaluable guidance. I am highly indebted for his encouragement and motivation throughout the course of this work. For his untiring cooperation, time and patience, this work would not have seen the light of the day.

“Every experience, every thought, every word, every person in your life is a part of a larger picture of your growth”. I express my thanks to my parents and friends especially to the members of the flight mechanics cell for their cooperation and moral support during the present work.

K. Venkat Chandra Sekhar  
Kanpur.

# CONTENTS

|  |            |
|--|------------|
| <b>Abstract</b>  | <b>iii</b> |
| <b>List of figures</b>   | <b>vii</b> |
| <b>List of tables</b>  | <b>ix</b>  |
| <b>Nomenclature</b>  | <b>x</b>   |
| <br>   |            |
| <b>Chapter 1 Introduction</b>  | <b>1</b>   |
| <b>Chapter 2 Generation of flight data</b>   | <b>13</b>  |
| 2.1 Ballistic Target   | 13         |
| 2.2 Aircraft   | 16         |
| 2.3 Short Range Strategic Missile  | 20         |
| 2.4 Artillery Shell  |            |
| 2.4.1 Point mass model   | 24         |
| 2.4.2 Modified point mass model  | 25         |
| 2.4.3 Six Degree of freedom model  | 26         |
| <br>   |            |
| <b>Chapter 3 Results and discussions</b>   | <b>31</b>  |
| 3.1 Estimation of ballistic coefficient from ballistic<br>target data (FD-BT)              | 31         |
| 3.2 Aircraft flight data (FD-AC)   | 32         |
| 3.3 Estimation using flight data of a typical short range strategic                        | 37         |
| 3.4 Estimation of aerodynamic parameters using flight data of a<br>typical artillery shell | 40         |
| 3.4.1 Estimation using point mass model  | 40         |
| 3.4.2 Estimation of aerodynamic parameters using MPM                                       | 46         |
| 3.4.2.1 Flight data simulated with constant<br>aerodynamic parameters                      | 46         |
| 3.4.2.2 Flight data simulated using aerodynamic<br>parameters varying with Mach number     | 46         |

|  |           |
|--|-----------|
| <b>Chapter 4 Conclusions and suggestions for future work</b> | <b>50</b> |
| 4.1 Conclusions  | 50        |
| 4.2 Suggestions for future work                              | 50        |
| <b>References</b>  | <b>52</b> |
| <b>Appendix A</b>  | <b>54</b> |
| <b>Appendix B</b>  | <b>57</b> |



# LIST OF FIGURES

| Fig. No. | Title   | Page No. |
|----------|---|----------|
| 1.1      | Output error method.  | 4        |
| 1.2      | Filtering approach.   | 5        |
| 1.3      | Filter error method.  | 7        |
| 2.1      | Forces acting on a one-dimensional ballistic target.                                      | 14       |
| 2.2      | Time histories of Ballistic Range data corresponding to $\beta=500\text{lb/ft}^2$ .       | 15       |
| 2.3a     | Elevator input type 1- Pulse input.   | 16       |
| 2.3b     | Elevator input type 1- 3-2-1-1 input.   | 16       |
| 2.4      | Simulated response $\alpha$ and $q$ for step input, without noise (FD-AC1).               | 18       |
| 2.5      | Simulated response $\alpha$ and $q$ for 3-2-1-1 input, without noise (FD-AC2).            | 19       |
| 2.6      | Simulated response $\alpha$ and $q$ for step input, with noise 10% (FD-AC1).              | 19       |
| 2.7      | Simulated response $\alpha$ and $q$ for 3-2-1-1 input, with noise 10% (FD-AC2).           | 20       |
| 2.8      | Measured variables with respect to time without noise (FD-SM).                            | 23       |
| 2.9a     | Typical measured data of X, Y, Z without noise.   | 29       |
| 2.9b     | Typical measured data of u, v, w without noise.   | 29       |
| 2.9c     | Typical measured data of p, q, r without noise.   | 30       |
| 3.1      | Convergence of estimated parameters with time for 3-2-1-1 input and 5% measurement noise. | 35       |
| 3.2      | Convergence of variance with time for 3-2-1-1 input and 5% measurement noise.             | 36       |
| 3.3      | Convergence of $C_d$ as plotted w.r.t. range , case1.                                     | 41       |
| 3.4a     | Comparison of measured and EKF predicted trajectories case1.                              | 42       |

|      |   |    |
|------|---|----|
| 3.4b | Error in range and height for case1.  | 42 |
| 3.5  | Convergence of $C_d$ as plotted w.r.t. range.   | 43 |
| 3.6a | Comparison of measured and EKF predicted trajectories.                                | 43 |
| 3.6b | Error in range and height.  | 43 |
| 3.7  | Convergence of $C_d$ as plotted w.r.t. range , case1.                                 | 44 |
| 3.8a | Comparison of measured and EKF predicted trajectories case1.                          | 45 |
| 3.8b | Error in range and height for case1.  | 45 |
| 3.9  | $C_d$ Vs Mach number for case2, FD-SDF.   | 46 |
| 3.10 | Estimation of constant parameters using MPM from FD-SDF.                              | 47 |
| 3.11 | Estimation of $C_d$ and $C_{lp}$ as a function of Mach number (45 degrees elevation). | 48 |

## LIST OF TABLES

| <b>Table No.</b> | <b>Title</b>   | <b>Page No.</b> |
|------------------|--|-----------------|
| 2.1              | Geometric/mass characteristics of aircraft.  | 17              |
| 2.2              | Aerodynamic characteristics of aircraft.   | 17              |
| 2.3              | Geometric/mass characteristics of Strategic Missile.   | 21              |
| 2.4              | Aerodynamic characteristics of Strategic Missile.  | 21              |
| 2.5              | Control surface deflection with time.  | 24              |
| 2.6              | Geometric characteristics of the artillery shell.  | 27              |
| 2.7              | Aerodynamic characteristics of the artillery shell.  | 28              |
| 3.1              | Comparison of estimates of ballistic coefficient obtained using both ML and EKF  | 31              |
| 3.2              | Comparison of aerodynamic parameters of obtained by using ML and EKF method on FD-AC1 and FD-AC2 with 5% measurement noise.              | 33              |
| 3.3              | Comparison of aerodynamic parameters obtained by using ML and EKF method on FD-AC1 and FD-AC2 with 10% measurement noise.                | 34              |
| 3.4              | Range of initial values for which ML method was able to estimate aerodynamic parameters of a Short range strategic missile..             | 38              |
| 3.5              | Comparison of estimated parameters (SM) obtained using ML and EKF method for different initial guess values and measurement noise of 5%. | 39              |
| 3.6              | Values of aerodynamic parameters used for simulation in case 1.  | 40              |

# NOMENCLATURE

|                    |   |
|--------------------|---|
| $C_L, C_{d0}, C_m$ | = Non-dimensional lift, drag and pitching moment coefficients.              |
| $C_{L0}, C_{m0}$   | = Non-dimensional lift, and pitching moment coefficients at $\alpha = 0$ .  |
| $C_N, C_A$         | = Coefficient of normal and axial force.                                    |
| $C_x, C_y, C_z$    | = Coefficient of longitudinal, lateral, vertical force.                     |
| $d$                | = Diameter of the artillery shell, mm.                                      |
| $g$                | = Acceleration due to gravity, $m/s^2$ .                                    |
| $I_x, I_y$         | = Moment of inertia about x and y axis, $kgm^2$ .                           |
| $m$                | = Mass of the shell, kg.  |
| $p$                | = Roll rate, rad/s.   |
| $q$                | = Pitch rate, rad/s.  |
| $\bar{q}$          | = Dynamic pressure, $N/m^2$ .   |
| $r$                | = Yaw rate, rad/s.  |
| $r_e$              | = Distance from earth center to C.G. of the shell, m.                       |
| $R$                | = Radius of earth, m.   |
| $R_{T2}$           | = Ballistic target range, ft.   |
| $V_{T2}$           | = Ballistic target velocity, ft/s.  |
| $s / S_{ref}$      | = Reference area of the artillery shell, aircraft/ballistic target, $m^2$ . |
| $t$                | = Time of flight, sec.  |
| $T$                | = Ballistic air temperature (ambient air temperature), $^{\circ}C$ .        |
| $u, v, w$          | = Velocity components in x, y and z body axes, m/s.                         |
| $V$                | = Total velocity, m/s.  |
| $W_x, W_y, W_z$    | = Head/tailwind, crosswind and vertical wind components, m/s.               |
| $x, y, z$          | = Spatial coordinates, m.   |
| $\alpha_r$         | = Yaw of repose.  |

|          |  |
|----------|--|
| $\omega$ | = Rotation vectors.  |
| $\Omega$ | = Earth rotation angular velocity, rad/s.                                      |
| $\rho$   | = Density of air, kg/m <sup>3</sup> .  |
| $\theta$ | = Firing Table Elevation, Pitch attitude, deg.                                 |
| $\phi$   | = Roll attitude, deg.  |
| $\psi$   | = Yaw angle, deg.  |
| $\alpha$ | = Angle of attack, deg.  |
| $\beta$  | = Ballistic target coefficient, lb/ ft <sup>2</sup> or Angle of sideslip, rad. |

### Superscripts

|   |                                    |
|---|------------------------------------|
| . | = Derivative with respect to time. |
| → | = Vector quantity.                 |

### Subscripts

|             |  |
|-------------|--|
| o           | = Initial conditions.                    |
| $x, y, z$   | = Components along x, y and z direction. |
| <i>wind</i> | = Wind axes.                             |

### Stability and control derivatives

$$\begin{aligned}
C_{L\alpha} &= \frac{\partial C_L}{\partial \alpha}, & C_{Lq} &= \frac{\partial C_L}{\partial (qd/2V)}, & C_{L\delta} &= \frac{\partial C_L}{\partial \delta}. \\
C_{m\alpha} &= \frac{\partial C_m}{\partial \alpha}, & C_{mq} &= \frac{\partial C_m}{\partial (qd/2V)}, & C_{m\delta} &= \frac{\partial C_m}{\partial \delta}. \\
C_{l\delta} &= \frac{\partial C_l}{\partial \delta}, & C_{lp} &= \frac{\partial C_l}{\partial (pd/2V)}. \\
C_{n\beta} &= \frac{\partial C_n}{\partial \beta}, & C_{nr} &= \frac{\partial C_n}{\partial (rd/2V)}. \\
C_{y\beta} &= \frac{\partial C_y}{\partial \beta}, & C_{yr} &= \frac{\partial C_y}{\partial (rd/2V)}.
\end{aligned}$$

## CHAPTER 1

# INTRODUCTION

Artillery forms an important wing of the army to provide firepower during war as well as during cross-border skirmishes with the enemy. Artillery generally falls into three basic categories: guns, howitzers and mortars. The principle difference between them being the trajectory of the round fired. A gun has a high muzzle velocity, and is normally used in a direct fire mode where the target can be seen and penetration is desirable. Howitzers have a somewhat lower muzzle velocity and arc their shells onto a target. They are used in both a direct fire and indirect fire mode. This is especially useful when an enemy is concealed behind a prepared position or the artillery men desire to have a shell explode over an enemy's head. The airburst does less damage to hardened targets, but causes many more human casualties due to shell fragmentation covering a large area. Mortars have a very pronounced arc of flight. They have a relatively low muzzle velocity and are unsuitable for direct fire. Their principle value comes from being able to lob shells behind an obstacle, such as a fortification or a hill. They are not very accurate and dependent upon the amount of propelling powder to determine the point of impact. ↗

The effectiveness of artillery is largely judged by the accuracy in hitting the targets. The accuracy and reliability is influenced by the design criteria used in designing the shell. Artillery shells are a class of projectiles around which much of the aeroballistic theory was originally developed, and they continue to form a significant part of the aeroballistician's interest.

Study of the motion of projectiles through an external medium is known by the name of external ballistics. If the external medium is the earth's atmosphere, then external ballistics become synonymous with aeroballistics.

The conventional approach hitherto for understanding the in-flight behaviour of projectiles was to develop mathematical models that could predict all elements of the trajectory from launch to target. For this purpose, it becomes essential that all forces, moments affecting the flight of the projectile be accounted for in a well-defined mathematical form<sup>1</sup>. Beginning with the most simple but relatively inaccurate mathematical model, the in-vacuo trajectory model, more and more sophisticated models of increasing accuracy such as the point mass model (PM), the modified point mass model (MPM) and the six-degrees-of-freedom (SDF) model have been developed<sup>1</sup>. These models require aerodynamic coefficients as input (e.g., drag coefficient  $C_d$ , damping in roll derivative  $C_{l_p}$ , lift curve slope  $C_{L\alpha}$ , etc.). Accurate values of these parameters are required in mathematical model for description of artillery shell dynamics.

There are three distinct approaches for estimating aerodynamic parameters:

- Theoretical methods
- Wind tunnel testing
- Flight-testing

At the preliminary design stage of any system, theoretical methods<sup>2,3,4</sup> are used in spite of their limited accuracy. Wind tunnel testing improves the accuracy of estimation but is a time consuming and expensive way of estimating aerodynamic parameters. Precise simulation of control surfaces, power effects of flight conditions is difficult. The model tested in the wind tunnel is generally slightly different from actual flight due to the last

minute configuration changes. Other reasons for discrepancies between flight and wind tunnel results are Reynolds number discrepancies and interferences due to support system. It is therefore desirable that the wind tunnel estimates be corroborated with the estimates from actual flight test data.

The most commonly used methods for parameter estimation from flight data are broadly classified into the following categories.

- Equation error methods
- Output error methods
- Filtering approach
- Filter-error methods
- Neural Network based methods.

The principle of Least squares is used in the equation error method wherein the error gets minimized with respect to the unknown parameters in each of the equations. Its advantages include computational simplicity, non-iterative nature and applicability to both linear and non-linear models. The disadvantage is that the method cannot be directly applied if all the states are not measured accurately, and produces poor results if the measurements are noisy. Therefore in order to get accurate results, considerable effort is required for data reconstruction and smoothing. Sometimes these data processing tasks are more complicated than the task of parameter estimation itself. However these methods are useful as startup for more advanced estimators.

In the output error method, the error between the measured and the model response is minimized. The method assumes that there exist no modelling errors. This method



processes the measurement noise while assuming the model representation of the given system to be exact. A comprehensive survey of these methods is reported by Maine and Iliff<sup>5</sup>. The methods like analog matching<sup>6</sup>, Newton Raphson method<sup>7</sup>, modified Newton Raphson method<sup>7</sup> etc. fall in this category. Maximum likelihood (ML) method is one of the variants of output error methods. Maximum Likelihood estimates are those for which the observed value would be the most likely to occur; “most likely” is defined as maximization of likelihood function of the observed responses, given the parameters. The main advantage of this method is that parameter estimates are asymptotically unbiased, consistent and efficient provided the model assumed is correct. The schematic block diagram of ML method is presented below through Fig 1.1 and algorithm is presented in Appendix B.

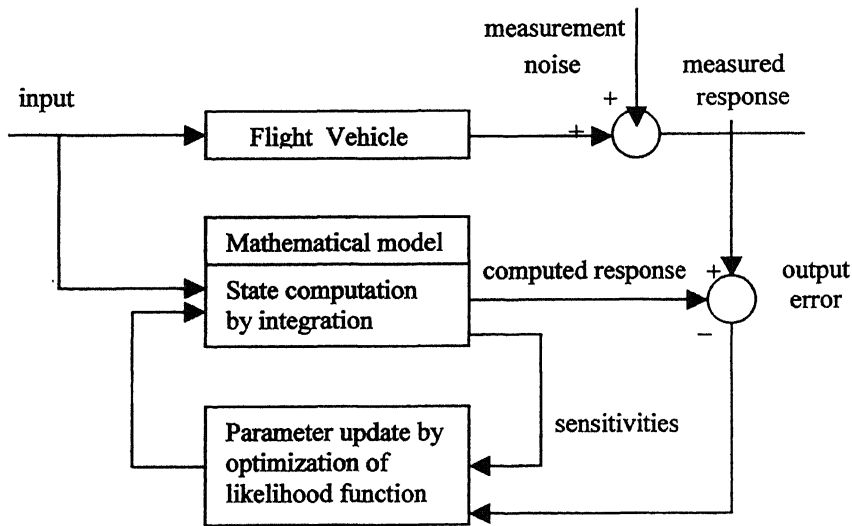


**Fig. 1.1 Output error method**

Filtering approach<sup>8,9</sup> is an extension of Kalman filter<sup>10,11</sup>. Kalman filter is a linear, optimal estimator of state variables of a linear, time-varying system, operating in a Gaussian stochastic environment. Optimal estimator here is referred to a computational

algorithm that processes measurements to deduce a minimum error covariance of the state of a system combining all the information available i.e.

- knowledge of system and measurement dynamics
- assumed statistics of system noise and measurement
- initial condition information.

Traditional Kalman filter is applicable and optimal for linear systems only. When either the system or the measurement equations are non-linear, the same algorithm can still be applied by local linearization the system about the current state. Such filter applied to nonlinear systems is called Extended Kalman Filter (EKF)<sup>8,9,12</sup>, and it need not be optimal. For Kalman filter to be used as a parameter estimator, the unknown parameters are added as additional state variables, by considering the constant system parameters vector as the output of an auxiliary dynamic system. Parameter estimation is inevitably a nonlinear estimation problem whether the system and measurement equations are linear or non-linear. The detailed description about Extended Kalman Filter is presented in Appendix A. The schematic block diagram of EKF is presented below through Fig. 1.2.

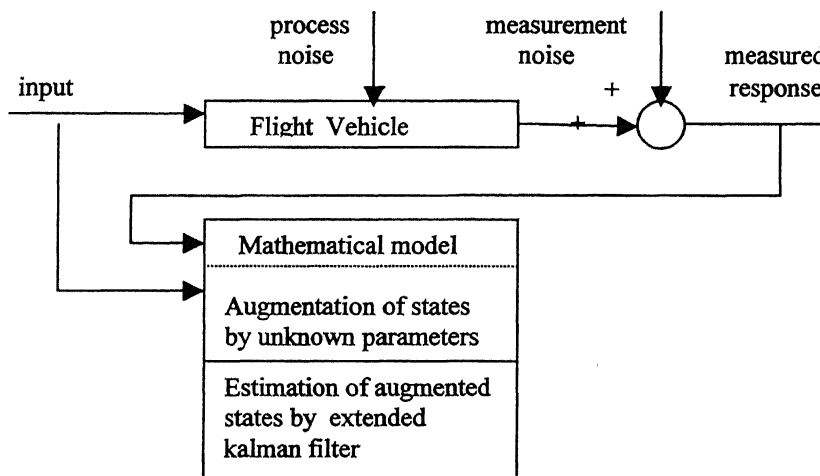


**Fig. 1.2 Filtering approach**

EKF produces estimates of the parameters that approximately minimize the mean square error in the parameter estimates themselves as opposed to minimizing a cost function that is based on matching the output variable behavior given a specific input trajectory, which is what most ML and least squares techniques do. This filtering approach is well suited for online applications, can handle process noise (modeling errors) and measurement noise (instrument errors). Extended Kalman Filter produces time histories for each of the estimated parameters, which is very useful if the time-varying nature of the parameters is of interest. But the performance of the filter strongly depends on the initial statistics of process noise, measurement noise and apriori covariance matrix. Information about the measurement noise covariance can be obtained from the laboratory calibration of measurement sensors used. Process noise is however more difficult to determine. Several procedures for obtaining measurement and process noise prior to estimation are available in literature. Well known methods by Mehra<sup>13</sup> and Morelli<sup>14</sup> are being used with partial success. Other kind of approach known as adaptive filtering adjusts the covariances during estimation. Myers and Tapley<sup>15</sup> gave one such algorithm of adaptive filtering/tuning. Extended Kalman Filter is only a first order minimum variance filter. The higher order terms neglected in the propagation of the error covariance can possibly lead to biased estimates. Various techniques such as iterated EKF(IEKF) or second and higher order filters are often used in many applications to reduce the estimation errors. In the present work no attempt has been made to use either adaptive filtering or higher order filters.

Filter error method<sup>8,9</sup> is the most general stochastic approach to parameter estimation, which accounts for both process and measurement noise. It can give good

estimates from data collected in turbulent atmosphere(process noise) also. In this direct approach an appropriately defined cost function, usually the statistically formulated likelihood function, is optimized with respect to the unknown parameters using some suitable optimization method. The Gauss Newton method is generally used for this purpose. Filter is used only for the natural purpose of obtaining the true state variables from the noisy measurements, i.e. for state estimation. The scheme describing this method is presented in Fig.1.3.

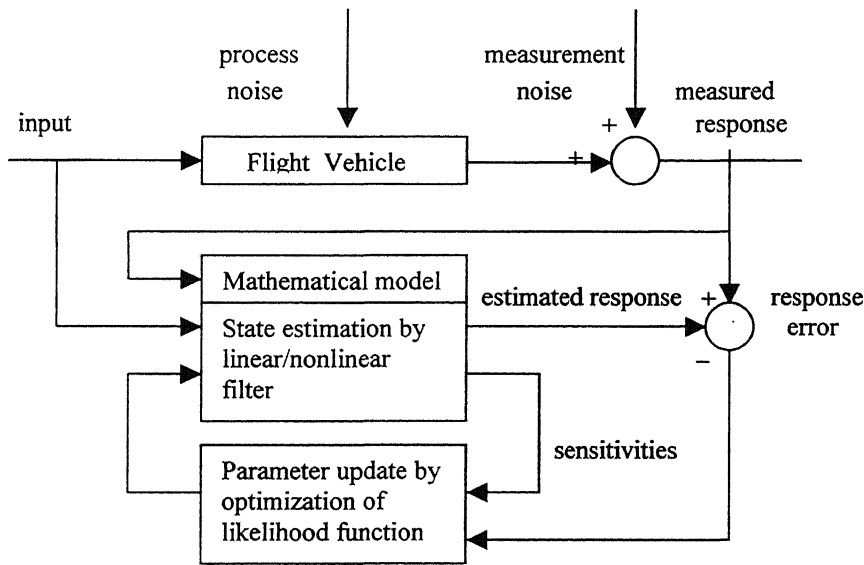


**Fig. 1.3 Filter error method**

Application of Artificial Neural Networks (ANNs) for flight vehicle modeling and parameter estimation is a relatively new emerging field<sup>8</sup>. We have reported works on application to aircraft, not yet to rockets and artillery shells. In this approach the aircraft motion variables and control inputs are mapped to predict the total aerodynamic coefficients. Of the various architectures of NN, two types namely Feed Forward Neural network (FFNN) and Reccurent Neural network (RNN) have found favour in parameter estimation. FFNNs lead to a black box type of modelling, where no physical significance

can be attached either to the network structure or to the weights. The weights or parameters of the network are estimated by the back propagation algorithm. On the other hand, RNNs are amenable to state space modeling. They have fixed number of mutually connected nodes equal to the number of unknown parameters of the postulated state space model. Partly due to the fixed structure and partly due to difficulties involved in tuning the sigmoidal nonlinearity of RNNs, FNNs found wider applications than RNNs.

Parameter estimation of an aircraft with many measurements like, acceleration (both linear and angular), angular orientation, speed, angle of attack etc. has been discussed in detail in Ref.8. But from cost effectiveness point of view (and also because of the non-availability of space for instrumentation), it may not be feasible to use many sensors for artillery shells going through many development flight trials.

As an alternative approach, limited flight tests are routinely conducted with scale down model in Aero-ballistic range facility<sup>16</sup>. The test facility is an enclosed, atmospheric, instrumented concrete structure used to examine the exterior ballistics of various free flight configurations. The facility contains gunroom, control room, model measurement room, blast chamber and instrumented range. The range may have large number of locations available as instrumentation sites. Each station is used to house fully instrumented orthogonal shadowgraph stations. Using this instrumentation, spatial positions, speed and angular orientations etc. are estimated. These are then used for parameter estimation.

Winchebach et al<sup>16</sup> conducted free flight aeroballistic tests to obtain subsonic and supersonic aerodynamic parameters of a wrap around fin configuration. The aerodynamic parameters presented were extracted from the position-attitude time histories of the

experimentally measured trajectories using non-linear numerical interpolation data reduction routines.

Defense Research Establishment, Quebec, Canada is currently engaged in research on high length/diameter ratio energy penetrators for 70mm air launched rocket application. One of the objectives of the program is to enlarge the free-flight aerodynamic database of high  $l/d$  finned projectiles<sup>17</sup>. Dupis investigated six model configurations (scale down) during the test program<sup>17</sup>. Standard SDF routine with ML method was used to match the theoretical trajectory to the experimentally measured trajectory. In that analysis, as a first step, the basic dynamic range data (time, position, angles), physical properties and atmosphere conditions were assembled and then SDF (with ML) were performed to estimate the aerodynamic parameters. The results of this analysis showed that once time histories of position, angles are recorded it is possible to estimate aerodynamic parameters using free flight test data.

It is worth mentioning that aerodynamic parameters are strong functions of Mach number. In order to capture this dependence on Mach number, projectiles are fired at different initial Mach number and the basic data corresponding to that Mach number are recorded and analyzed for parameter estimation. Though this approach looks attractive (if such facility is available), however it has the following two distinct limitations:

- 1) It may not be possible to simulate actual flight path that the full-scale model would be traversing.
- 2) It requires large number of firings to capture Mach number dependence of aerodynamic parameters.

In view of the above, there have been conscious efforts towards generation of flight data of free flight projectile by simultaneous measurements with pulse radar or optical system for position data and continuous wave Doppler radar for velocity measurements. In order to improve the overall accuracy several systems of each type have often been used in parallel. However, this complicated and very expensive set up is not required today. From a single continuum wave Monopulse Azimuth and Elevation Doppler Tracking Radar it is possible to extract highly accurate velocity and position data in three dimensions without any assumptions of ballistic behavior.

Defense Research Organization of India, is currently engaged in design and development of new artillery shell, rockets etc. There is a routine demand for post flight analysis of flight data. In particular, there is strong demand for estimation of aerodynamic parameters from flight data to validate the design as well as to prepare database for fire control system (FCS) to enhance artillery effectiveness. Accurate values of aerodynamic parameters are of paramount importance in building effective FCS.

In the present work, ML and EKF method are used for parameter estimation purposes. The motivation here was to conduct a study on the applicability of these methods in extracting aerodynamic parameters by processing flight data obtained for different class of flight vehicle/store. These methods have been applied to flight data starting from a one-dimensional ballistic target to, an artillery shell, longitudinal motion of Short Range Strategic Missile (SM) and also to flight data of an aircraft. As discussed earlier, the flight data obtained through aircraft maneuvers contain large number of information regarding its motion and control variables. This is possible because exhaustive instrumentation for data acquisition is possible for such aircraft. Flight data of

one-dimensional ballistic target contain very limited information regarding its motion/control variables. Same is the case for flight data obtained through radar tracking the spatial coordinates and velocity of a shell/rocket in flight. Any parameter estimation method requires adequate information about vehicle dynamics to estimate aerodynamic parameters correctly. Unlike flight data of aircraft, others (rockets/shells) face this problem of lack of information content in relation to estimation of aerodynamic parameters. Thus challenges remain at place to evolve strategies to estimate aerodynamic parameters using such data of limited information content. This study systematically explores the possibility of applying the methods to estimate aerodynamic parameter under such constraints. Further, the flight data obtained through typical strategic missile vehicle has some flavour of both aircraft and rocket/shell. A strategic guided missile has control surfaces, lifting surfaces and is generally housed with more number of sensors like accelerometers, gyros etc. as compared to none for shell or rocket. Thus a typical flight data obtained through such flight vehicle have more information content as compared to free flight rockets or shells. However, excitation of such missiles with best control input (for the purpose of parameter estimation) may not always be feasible, where as it is always a routine task to generate flight data with such input for aircraft. Hence information content available with such missile data though superior in comparison to free flight rockets/shells but is many fold inferior as compared to aircraft flight data.

The applicability of the existing methods (ML and EKF) is tested for these three different classes of flight data. It is observed that both ML and EKF can be advantageously applied to estimate few aerodynamic parameters with acceptable level of accuracy.



Chapter 2 describes methodologies used to generate flight data for type of vehicle considered. In chapter 3 results and discussions are presented and chapter 4 concludes with scope for future work.

## CHAPTER 2

# GENERATION OF FLIGHT DATA

Due to the non-availability of real flight data, simulated flight data are generated for the purpose of parameter estimation. Mathematical models used to generate flight data of ballistic target, aircraft longitudinal motion, Short Range Strategic Missile(SM) and artillery shell are presented in subsequent paragraphs.

### 2.1 Ballistic target

Knowledge of target ballistic coefficient can be used in advance guidance laws such as predictive guidance to relax the interceptor acceleration requirements. In addition, knowledge of the target ballistic coefficient is required for fire control due to the importance of accurate intercept point predictions in launching the interceptor on a collision course. Therefore, accurate estimation of ballistic coefficient of a target re-entering the atmosphere is very important for both guidance and fire control purposes. The flight data for simulating such a vehicle motion is modelled to investigate the applicability of both ML and EKF method<sup>18</sup> in extracting parameter (ballistic coeff) from flight data.

To generate flight data, one dimensional motion has been considered<sup>18</sup>. In this example it is assumed that a ballistic target is falling on a straight line path directly towards a surface-based tracking radar. Only drag and gravity force acting on the ballistic target have been modeled.

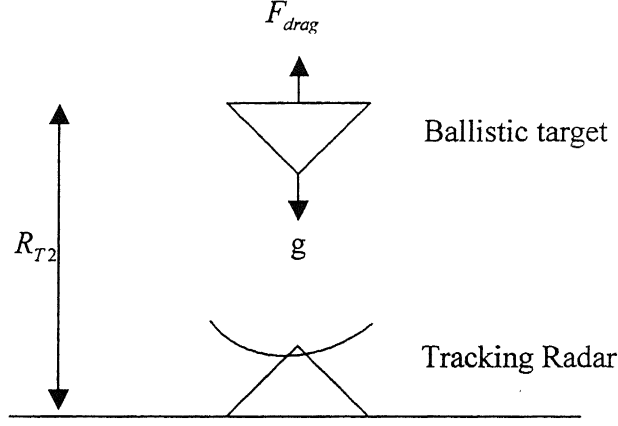


**Figure 2.1 Forces acting on a one-dimensional ballistic target.**

In this problem, the tracking radar measures the distance from the radar to target every  $T_s$  seconds. Referring to Fig. 2.1, it can be seen that the drag acts upwards whereas gravity acts downward. The total acceleration acting on the ballistic target can be expressed in terms of a zero lift drag  $C_{D0}$  or a ballistic coefficient,  $\beta$ , as

$$\frac{dV_{T2}}{dt} = \frac{F_{drag}}{m} - g = \frac{\bar{q}S_{ref}C_{D0}}{W} - g = \frac{\bar{q}g}{\beta} - g \quad (2.1)$$

where  $\beta = \frac{W}{S_{ref}C_{D0}}$ ,  $g$  is the acceleration of gravity and  $\bar{q}$  is the dynamic pressure. The dynamic pressure can be expressed in terms of the air density  $\rho$  and ballistic target velocity  $V_{T2}$  as

$$\bar{q} = 0.5\rho V_{T2}^2 \quad (2.2)$$

For the purpose of simplicity, we can assume that the air density varies exponentially with height and its variation is modelled using the following relation,

$$\rho = \rho_0 e^{-R_{T2}} \quad (2.3)$$

Therefore two differential equations that govern the one dimensional ballistic target can be summarized as

$$\dot{R}_{T2} = V_{T2} \quad (2.4a)$$

$$\dot{V}_{T2} = \frac{0.0034e^{\frac{R_{T2}}{22000}} g V_{T2}^2}{2\beta} - g \quad (2.4b)$$

These equations were solved using 2nd order Runge-Kutta numerical integration technique. The relevant parameter (ballistic coefficient) used to generate the ballistic target flight data has been assumed to be  $500 \text{ lb/ft}^2$ . Time histories of range ( $R_{T2}$ ), which will be referred as Ballistic Target Range data (FD-BT) for future reference and is presented in Fig. 2.2. This will be treated as measured flight data. This data will be processed using both ML and EKF method to estimate relevant aerodynamic parameter (ballistic coefficient).

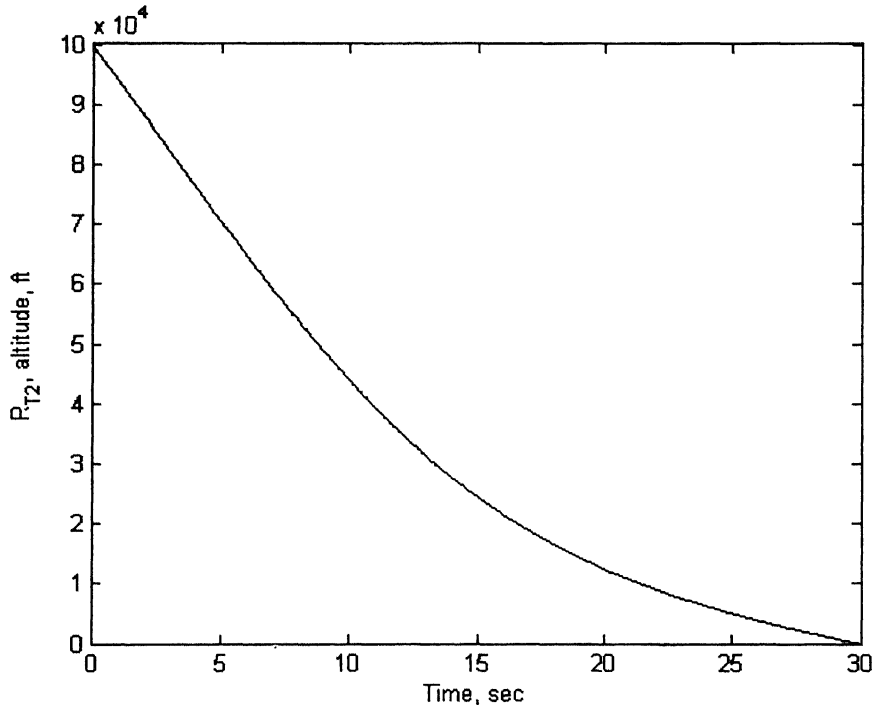


**Figure 2.2 Time histories of Ballistic Range data corresponding to  $\beta=500\text{lb/ft}^2$ .**

## 2.2 Aircraft

Knowledge of aerodynamic parameters are of paramount importance in postulating mathematical models for aircraft dynamics. Aircraft dynamics is generally dominated by two modes namely, longitudinal mode and lateral-directional mode. Longitudinal mode can have both short period( $u=\text{constant}$ ) and phugoid( $\alpha=\text{constant}$ ) modes. In this exercise, only short period excitation is considered. For short period mode accurate values of at least eight aerodynamic parameters are required to describe its dynamics. The relevant aerodynamic parameters are  $C_{L_0}, C_{L_\alpha}, C_{L_q}, C_{L_\delta}, C_{m_0}, C_{m_\alpha}, C_{m_q}$  and  $C_{m_\delta}$ . In order to estimate these parameters, it is necessary to excite the airplane in its longitudinal mode by perturbing the aircraft with external input of a particular type. Elevator input could be of various types; pulse, double pulse or specifically designed 3-2-1-1 input. Excitation using 3-2-1-1 input enhance information content in the flight data<sup>8,9</sup>. Typical elevator inputs used for simulating aircraft flight data (FD-A) are presented in Fig. 2.3(a) and Fig. 2.3(b).

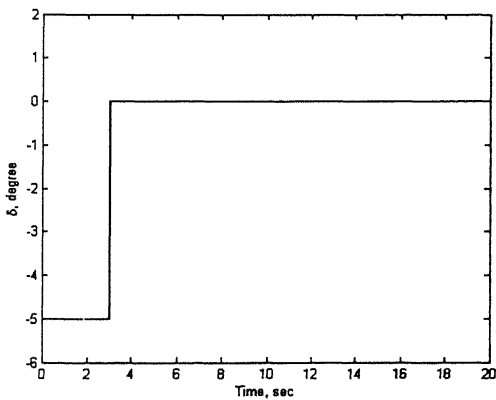


**Fig. 2.3(a) Elevator input type1**  
**Pulse input.**

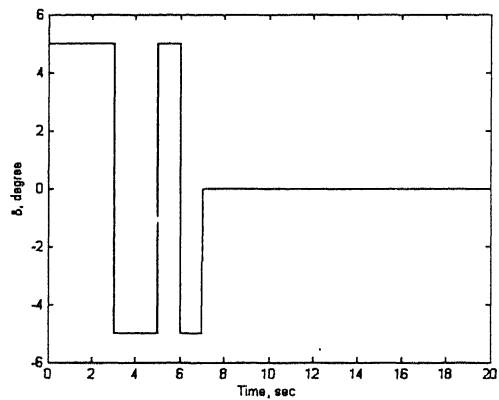


**Fig. 2.3(b) Elevator input type2**  
**3-2-1-1 input.**

The mathematical model used for simulating short period perturbed longitudinal mode is given below<sup>19</sup>.

$$\dot{\alpha} - q = -\frac{\rho u s}{2m} C_L \quad (2.5)$$

$$\dot{q} = \frac{\rho u^2 s c}{2I_y} C_m \quad (2.6)$$

where the assumed aerodynamic model is given by

$$C_L = C_{L_0} + C_{L_\alpha} \cdot \alpha + C_{L_q} \cdot (qc/2u) + C_{L_\delta} \cdot \delta$$

$$C_m = C_{m_0} + C_{m_\alpha} \cdot \alpha + C_{m_q} \cdot (qc/2u) + C_{m_\delta} \cdot \delta$$

Short period equations of motion were solved using 4<sup>th</sup> order Runge-Kutta method. The geometric, inertia and flight conditions used to generate simulated data are given in Table 2.1. The values of aerodynamic parameters used for generating simulated flight data are presented in Table 2.2.

**Table 2.1 Geometric/mass characteristics of aircraft.**

| SL.No. | Geometric/mass characteristics                |
|--------|---|
| 1.     | Chord length : 5.6m.                          |
| 2.     | Wing surface area : 38.40 m <sup>2</sup> .    |
|        | Mass : 9227.40 kg.                            |
| 3.     | I <sub>y</sub> : 67935.39 kg-m <sup>2</sup> . |
| 4.     | Speed : 61.72 m/s                             |

**Table 2.2 Aerodynamic characteristics of aircraft.**

| $C_{L_0}$ | $C_{L_\alpha}$ | $C_{L_q}$ | $C_{L_\delta}$ | $C_{m_0}$ | $C_{m_\alpha}$ | $C_{m_q}$ | $C_{m_\delta}$ |
|-----------|----------------|-----------|----------------|-----------|----------------|-----------|----------------|
| -0.0522   | 2.6307         | 4.4134    | 1.0425         | -0.0163   | -1.16          | -1.1228   | -0.3557        |

Time histories of angle of attack and pitch rate corresponding to various elevator input are presented in Fig 2.4 and 2.5 and are termed as FD-AC1 for elevator input type 1, and FD-AC2 for elevator input type 2. Time histories of  $\alpha$ ,  $q$  will be processed using ML and EKF method to estimate aerodynamic parameters. Further, the simulated flight data with varied degrees of measurement noise were also used to check the robustness of the methods. Fig. 2.6 and 2.7 present graphically the FD-AC with 10% noise to be used for estimation purpose.

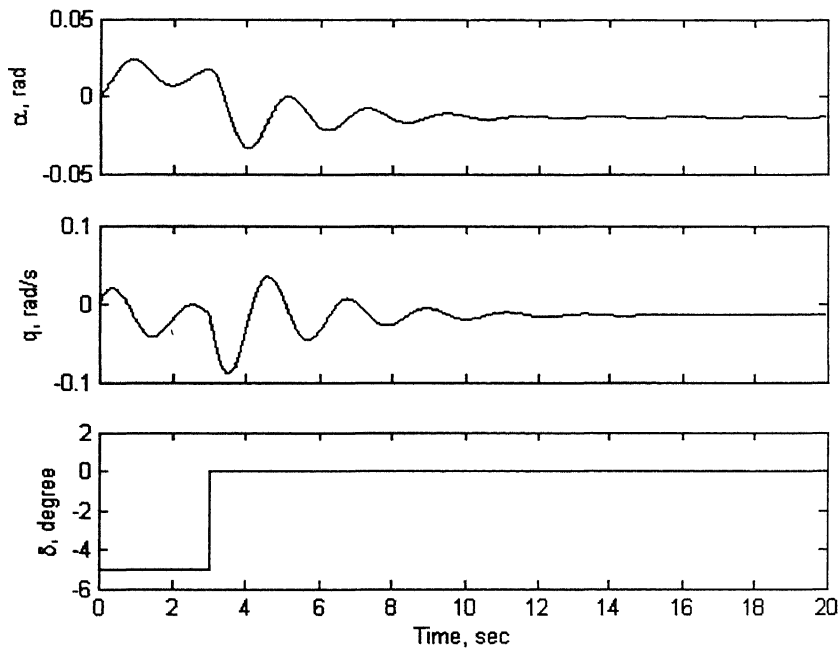


**Figure 2.4 Simulated response  $\alpha$  and  $q$  for step input, without noise (FD-AC1).**

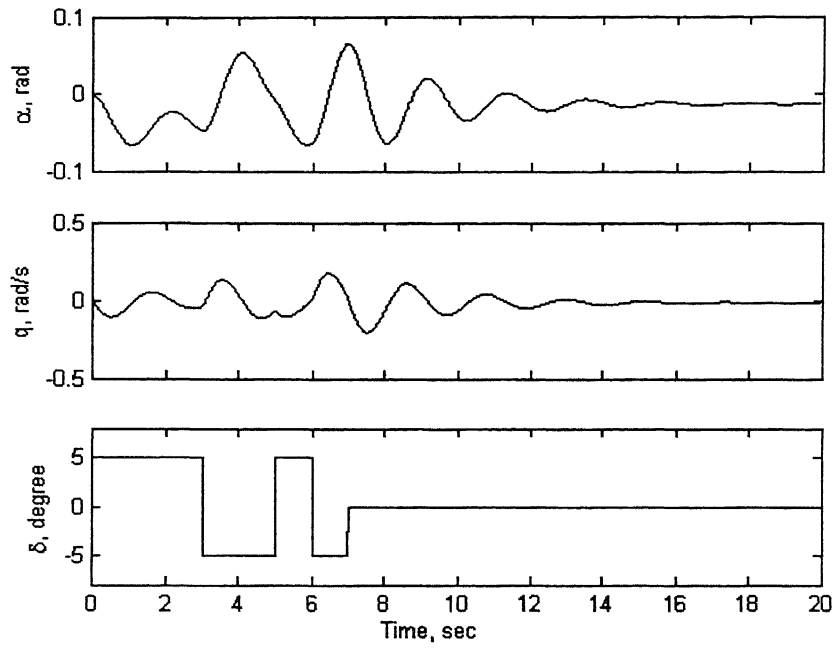


**Figure 2.5 Simulated response  $\alpha$  and  $q$  for 3-2-1-1 input, without noise (FD-AC2).**

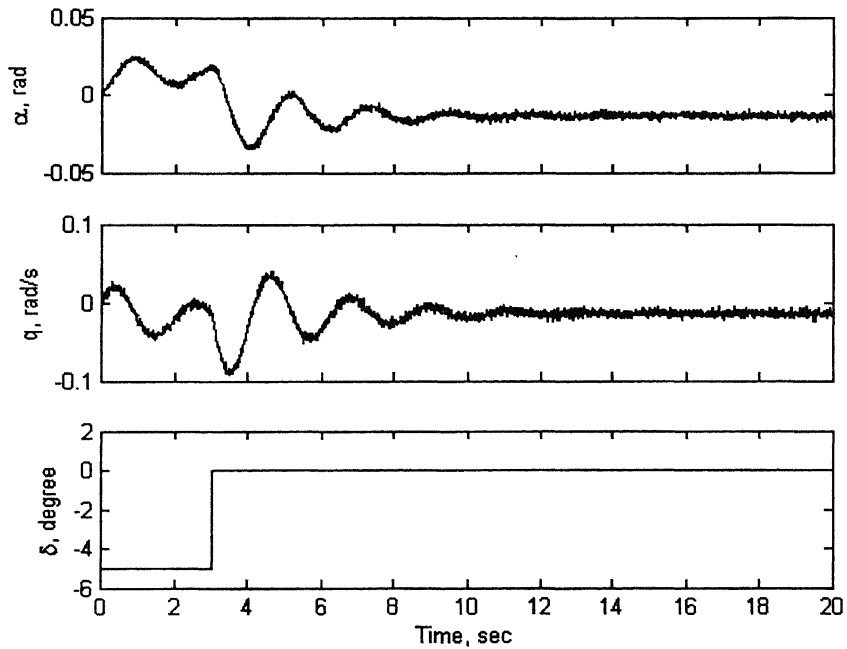


**Figure 2.6 Simulated response  $\alpha$  and  $q$  for step input, with noise 10% (FD-AC1).**



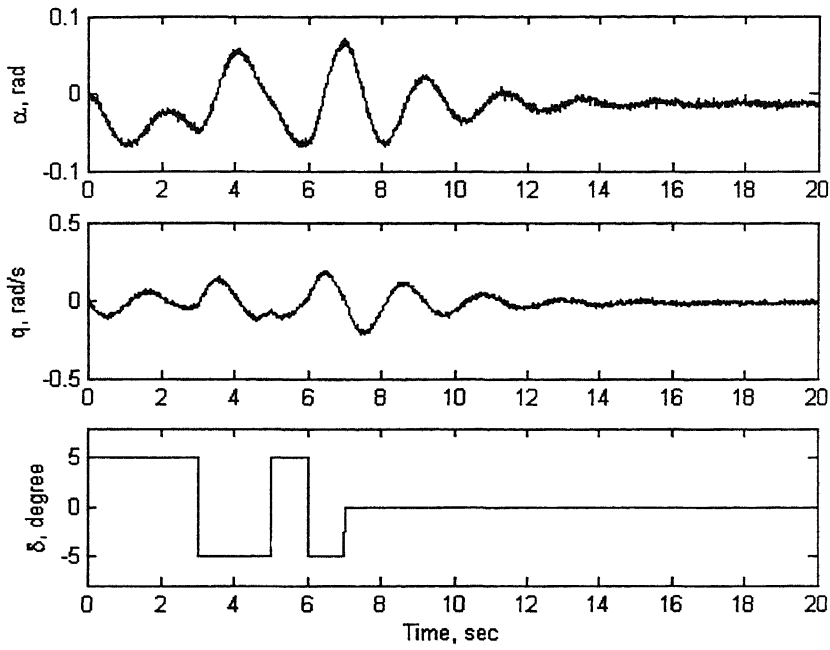


**Figure 2.7 Simulated response  $\alpha$  and  $q$  for 3-2-1-1 input, with noise 10% (FD-AC2).**

### 2.3 Short Range Strategic Missile (SM)

Strategic Missiles are generally used for short range (2-4 km) engagements. It has three distinct phases of flight path. It has to climb to reach a particular height, cruise for certain distance and then finally hit the target under the commanded guidance and control. In this work the third phase is taken to be a ballistic trajectory i.e., without guidance. It is initially propelled with high thrust, and subsequently after certain period of time, sustainer (with much lower thrust) takes over for a desired period of time. However, during the initiation of guidance and control, the missile is without any active thrust. In order to achieve predefined flight path, a set of preset control inputs are applied. The dynamics of this motion has been modeled using SDF trajectory model. In this study only the longitudinal motion is being considered. The equations representing SDF model are

listed in the subsequent section. The mass, moment and aerodynamic characteristics used to solve these equations of motion are listed in Table 2.3 and Table 2.4 respectively.

**Table 2.3 Geometric/mass characteristics of Strategic Missile.**

| SL.No. | Geometric/mass characteristics           |
|--------|--|
|        | Length/Dia : 8.33.                       |
|        | Mass, initial/final : 1.258.             |
|        | I <sub>x</sub> , initial/final : 1.2325  |
|        | I <sub>y</sub> , initial/final : 1.1657. |
|        | I <sub>z</sub> , initial/final : 1.1657. |

**Table 2.4 Aerodynamic characteristics of Strategic Missile.**

| $C_d$ | $C_{L_\alpha}$ | $C_{L_\delta}$ | $C_{m_\alpha}$ | $C_{m_\delta}$ |
|-------|----------------|----------------|----------------|----------------|
| 0.3   | 5.0            | 2.35           | -6.5           | -8.9           |

The Six degrees of freedom model used to represent the dynamics of SM is modeled using the following sets of equations as presented below.

$$\dot{u} = (\bar{q}s/m) C_x - q w + r v - g \sin \theta + (Th/m) \quad (2.7)$$

$$\dot{v} = (\bar{q}s/m) C_y - r u + p w + g \sin \phi \cos \theta \quad (2.8)$$

$$\dot{w} = (\bar{q}s/m) C_z - p v + q u + g \cos \phi \cos \theta \quad (2.9)$$

$$\dot{p} = \left\{ \bar{q}s d C_l + q r (I_y - I_z) \right\} / I_x \quad (2.10)$$

$$\dot{q} = \left\{ \bar{q}s d C_m + r p (I_z - I_x) \right\} / I_y \quad (2.11)$$

$$\dot{r} = \left\{ \bar{q}s d C_n + p q (I_x - I_y) \right\} / I_z \quad (2.12)$$

$$\dot{\phi} = p + q \tan \theta \sin \phi + r \tan \theta \cos \phi \quad (2.13)$$

$$\dot{\theta} = q \cos \phi - r \sin \phi \quad (2.14)$$

$$\dot{\psi} = r \cos \phi \sec \theta + q \sin \phi \sec \theta \quad (2.15)$$

To derive the spatial position equations, above equations were used to transform the body-axis velocity  $(u, v, w)$  into earth fixed axis. The equations are:

$$\begin{aligned} \dot{X} = & u \cos \psi \cos \theta + v (\cos \psi \sin \theta \sin \phi - \sin \psi \cos \phi) \\ & + w (\cos \psi \sin \theta \cos \phi + \sin \psi \sin \phi) + W_x \end{aligned} \quad (2.16)$$

$$\begin{aligned} \dot{Y} = & u \sin \psi \cos \theta + v (\sin \psi \sin \theta \sin \phi + \cos \psi \cos \phi) \\ & + w (\sin \psi \sin \theta \cos \phi - \cos \psi \sin \phi) + W_y \end{aligned} \quad (2.17)$$

$$\dot{Z} = u \sin \theta - v \cos \theta \sin \phi - w \cos \theta \cos \phi + W_z \quad (2.18)$$

Aerodynamic model used in this analysis is as given below:

$$Cx = -C_{Dwind} \cos \alpha \cos \beta + C_L \sin \alpha - C_{ywind} \cos \alpha \sin \beta$$

$$Cy = C_{ywind} \cos \beta - C_{Dwind} \sin \beta$$

$$Cz = -C_L \cos \alpha - C_{Dwind} \sin \alpha \cos \beta - C_{ywind} \sin \alpha \sin \beta$$

where,

$$C_L = C_{L0} + C_{L\alpha} \alpha + C_{Lq} (qd/2V) + C_{L\delta} \delta$$

$$C_{ywind} = C_{y0} + C_{y\beta} \beta + C_{yr} (rd/2V)$$

$$C_{Dwind} = C_d$$

$$C_i = C_{ip} (pd/2V)$$

$$C_m = C_{m0} + C_{m\alpha} \alpha + C_{mq} (qd/2V) + C_{m\delta} \delta$$

$$C_n = C_{n0} + C_{n\beta} \beta + C_{nr} (rd/2V)$$

Wind model used in this analysis is as given below:

$$u' = u - W_x \cos \theta \cos \psi - W_y \cos \theta \sin \psi + W_z \sin \theta$$

$$v' = v - W_x (\cos \psi \sin \theta \sin \phi - \sin \psi \cos \phi) \\ - W_y (\cos \psi \cos \phi + \sin \psi \sin \theta \sin \phi) \\ - W_z \cos \theta \sin \phi$$

$$w' = w - W_x (\cos \psi \sin \theta \cos \phi + \sin \psi \sin \phi) \\ - W_y (\sin \psi \sin \theta \cos \phi - \cos \psi \sin \phi) \\ - W_z \cos \theta \cos \phi$$

$$\text{thus, } \alpha = \tan^{-1} \left( \frac{w'}{u'} \right) \text{ and } \beta = \tan^{-1} \left( \frac{v'}{u'} \right)$$

where  $W_x, W_y, W_z$  are the wind components blowing toward the  $x, y$ , and  $z$  directions.

The flight data so generated corresponding to the elevator input as given in Table 2.5 are pictorially presented in Fig. 2.8. This flight data will be referred as FD-SM while estimating parameters from flight data representing flight of a short range strategic missile.

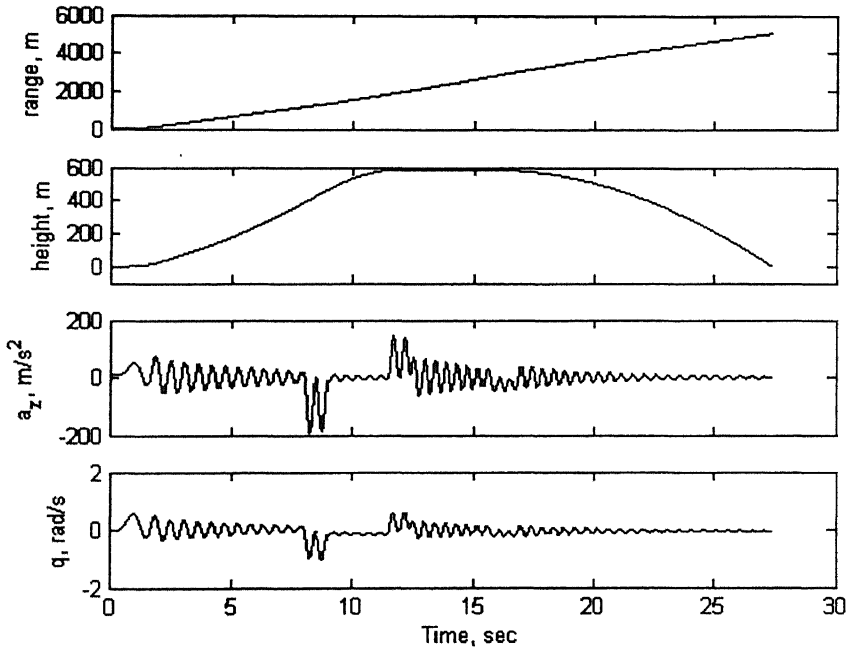


**Figure 2.8 Measured variables with respect to time without noise (FD-SM).**

**Table 2.5 Control surface deflection with time.**

| <b>Time interval</b> | <b>Control surface deflection, degrees</b> |
|----------------------|--|
| $0 < t < 8.5$        | -10.6                                      |
| $8.5 < t < 16.25$    | 10.0                                       |
| $12 < t < 16.25$     | -4.5                                       |
| $16.25 < t$          | 0.0  |

## **2.4 Artillery shell**

In general, the trajectory followed by center of mass of artillery shell in space is three-Dimensional  $(x, y, z)$ . Theoretical modelling of such trajectory demands aerodynamic modeling to be exhaustive. It requires usage of large number of aerodynamic parameters. Hence estimation of all parameters at one time might be involved. Initially in estimation algorithm only Point Mass Model (PM) was considered and as the work progressed , the trajectory model was made 3-Dimensional using Modified Point Mass Model (MPM) and Six Degree of Freedom model (SDF) respectively.

### **2.4.1 Point Mass Model (PM)**

In this model, it is assumed that the only aerodynamic force acting on the projectile is drag. It provides fairly accurate estimates of range for adequately stable projectiles and can also be used to estimate the first order effects of wind. The equations of motion for point mass model are given as below:

$$\frac{d^2x}{dt^2} = -\frac{\pi \rho d^2 C_d}{8m} V \left( \frac{dx}{dt} - W_x \right), \quad (2.19)$$

$$\frac{d^2y}{dt^2} = -g - \frac{\pi \rho d^2 C_d}{8m} V \left( \frac{dy}{dt} - W_y \right), \quad (2.20)$$

$$\frac{d^2z}{dt^2} = -\frac{\pi \rho d^2 C_d}{8m} V \left( \frac{dz}{dt} - W_z \right). \quad (2.21)$$

where  $x$  denotes range,  $y$  denotes height,  $z$  denotes drift and  $W_x$ ,  $W_y$ ,  $W_z$  respectively, the  $x$ ,  $y$  and  $z$  components of the wind velocity  $W$ . This model, however, does not account for the effect of spin of the shell and thus fails to predict the drift due to yaw of repose moment. Also, it neglects the lift forces acting on the shell.

#### 2.4.2 Modified Point Mass Model (MPM)

The modified point mass model is also known as four degree-of-freedom model (three spatial degrees-of-freedom plus axial spin). Its basis is a conventional point mass model, in addition, the instantaneous equilibrium yaw is calculated at each time step along the trajectory so as to provide estimates of yaw, drag, and drift resulting from the yaw of repose. The equations of motion for modified point mass model are given as below<sup>1</sup>:

$$\begin{aligned} \frac{d\bar{u}}{dt} &= -\frac{\pi \rho d^2}{8m} \left( C_{d0} + C_{d\alpha^2} \alpha_r^2 \right) v \bar{V} & (\text{Drag}) \\ &+ \frac{\pi \rho d^2}{8m} C_{L\alpha} v^2 \alpha_r & (\text{Lift}) \\ &- g_0 \frac{R^2}{r_e^3} \bar{r} - 2 \left( \bar{\omega} \times \bar{u} \right) & (\text{Gravity and Coriolis}) \end{aligned} \quad (2.22)$$

$$\frac{dp}{dt} = \frac{\pi \rho d^4}{16 I_x} p v C_{lp} \quad (\text{Spin damping}) \quad (2.23)$$

$$\alpha_r = \frac{-8p I_x}{\pi \rho d^3 C_{m\alpha}} \frac{[\vec{V} \times (d\vec{u}/dt)]}{v^4} \quad (\text{Yaw of repose}) \quad (2.24)$$

The quantities in the above equations are defined as follows:

$$\vec{u} = \frac{d\vec{x}}{dt}, \quad \vec{V} = \vec{u} - \vec{W}, \quad \vec{r} = \vec{x} - \vec{R}$$

$$\vec{R} = (0, -R, 0), \quad [\vec{W} \text{ Denotes the wind vector}]$$

$$\omega = (-\Omega \cos[\text{latitude}] \cos[\text{azimuth}], -\Omega \sin[\text{latitude}], \Omega \cos[\text{latitude}] \sin[\text{azimuth}])$$

where,  $\Omega = 7.29 \times 10^{-5} \text{ rad / s.}$  (rotation of the earth),

$R = 6370320 \text{ m}$  (radius of the earth),

$$g_0 = 9.80665 [1 - 0.0026373 \cos (2 \times \text{latitude}) + 0.0000059 [\cos (2 \times \text{latitude})]^2],$$

the axis system is as for the point mass model with  $\vec{x}$  being along the line of fire.

As may be seen from the above equations, the aerodynamic coefficient input required is extensive and accuracy of these aerodynamic coefficients is crucial for reliable estimates of range. However, for most artillery shells, the reliability of estimated values of aerodynamic coefficients is not high enough to inspire confidence in resulting range estimates from this model. In spite of this limitation, this model has the capability of providing reasonable accounts of end point data. It can estimate wind corrections and can accept non-linear aerodynamic inputs if required.

### 2.4.3 Six Degree of Freedom model (SDF)

The most sophisticated trajectory model developed was the six-degree-of-freedom model having the spatial degrees of freedom, yaw degree of freedom in two planes and the spin. In this model there are no assumptions concerning linearized aerodynamics or projectile symmetry. However, the indeterminability of many of the initial conditions and

aerodynamic coefficients which are required as input frequently results in the model not giving significantly better end results than the modified point mass model. Thus its usage might not be justified for routine fire control work. It is nevertheless a powerful tool for the ammunition designer. The equations of motion for six-degree-of-freedom model are as given for Strategic Missile except a small change in aerodynamic modeling. Here the aerodynamic modeling doesn't include the aerodynamic derivatives due to control surface deflection  $\delta$  as there are no control surfaces attached to shell. The description of SDF model has already been presented in section 2.3. The mass and aerodynamic characteristics of the artillery shell used in generating flight data are Table 2.6 and 2.7 respectively.

**Table 2.6 Geometric characteristics of the artillery shell.**

| SL. No. | Geometric characteristics  |
|---------|--|
| 1.      | Total length : 825 mm.   |
| 2.      | CG location : 533 mm from nose tip.  |
| 3.      | Diameter : 155 mm.   |
| 4.      | Mass : 42.6 kg.  |
| 5.      | Moment of Inertia<br>Axial, $I_{xx}$ : 0.146 kg-m <sup>2</sup> .<br>Traverse, $I_{yy}$ : 1.709 kg-m <sup>2</sup> . |



**Table 2.7 Aerodynamic characteristics of the artillery shell.**

| SL. No. | Mach Number | $C_d$ | $C_{m\alpha}$ | $C_{L\alpha}$ | $C_{lp}$ |
|---------|-------------|-------|---------------|---------------|----------|
| 1.      | 0           | 0.13  | 3.2           | 1.3           | -0.037   |
| 2.      | 0.85        | 0.13  | 3.2           | 1.3           | -0.031   |
| 3.      | 0.9         | 0.13  | 3.25          | 1.2           | -0.03    |
| 4.      | 0.92        | 0.14  | 3.3           | 1.1           | -0.03    |
| 5.      | 0.96        | 0.203 | 3.45          | 0.95          | -0.03    |
| 6.      | 0.98        | 0.269 | 3.5           | 0.95          | -0.03    |
| 7.      | 1           | 0.329 | 3.5           | 1             | -0.0297  |
| 8.      | 1.02        | 0.351 | 3.4           | 1.1           | -0.0295  |
| 9.      | 1.05        | 0.367 | 3.25          | 1.55          | -0.029   |
| 10.     | 1.1         | 0.366 | 3.15          | 1.85          | -0.029   |
| 11.     | 1.15        | 0.353 | 3.15          | 1.95          | -0.0285  |
| 12.     | 1.2         | 0.343 | 3.14          | 2             | -0.0282  |
| 13.     | 1.3         | 0.326 | 3.13          | 2.07          | -0.028   |
| 14.     | 1.4         | 0.314 | 3.12          | 2.15          | -0.027   |
| 15.     | 1.6         | 0.293 | 2.75          | 2.2           | -0.026   |
| 16.     | 1.8         | 0.273 | 2.5           | 2.3           | -0.025   |
| 17.     | 2           | 0.257 | 2.48          | 2.32          | -0.024   |
| 18.     | 2.2         | 0.245 | 2.47          | 2.35          | -0.023   |
| 19.     | 2.4         | 0.236 | 2.45          | 2.35          | -0.022   |
| 20.     | 2.6         | 0.229 | 2.4           | 2.35          | -0.0215  |

It may be mentioned that the flight data used for parameter estimation (for shell) was simulated using SDF model. A typical flight data showing X,Y,Z,u,v,w,p,q, and r has been presented in Fig. 2.9. However during estimation depending upon the number of

aerodynamic parameters to be estimated, selectively PM, MPM, SDF models were used.

The flight data for artillery shells will be referred by FD-SDF for future reference.

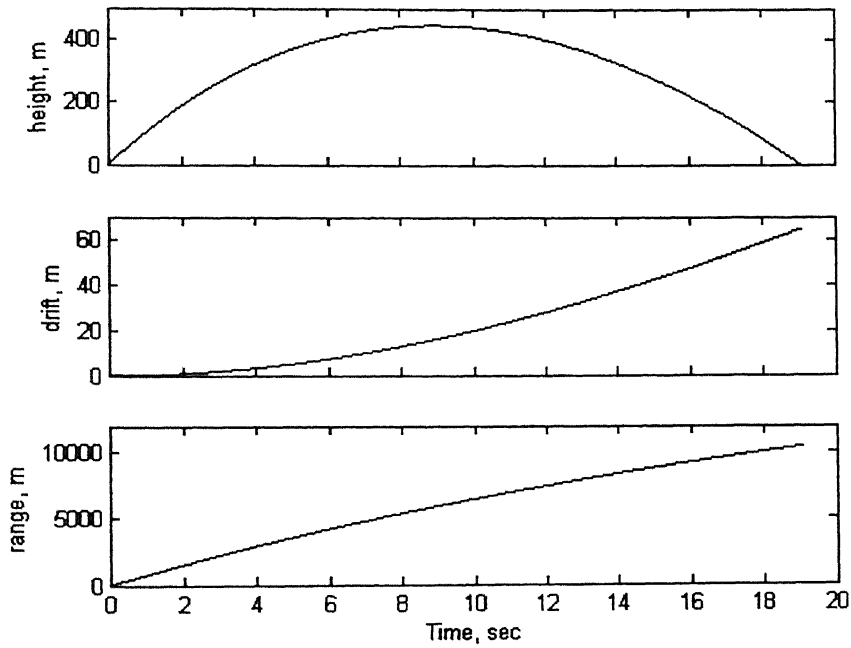


**Fig. 2.9a Typical measured data of X, Y, Z without noise.**

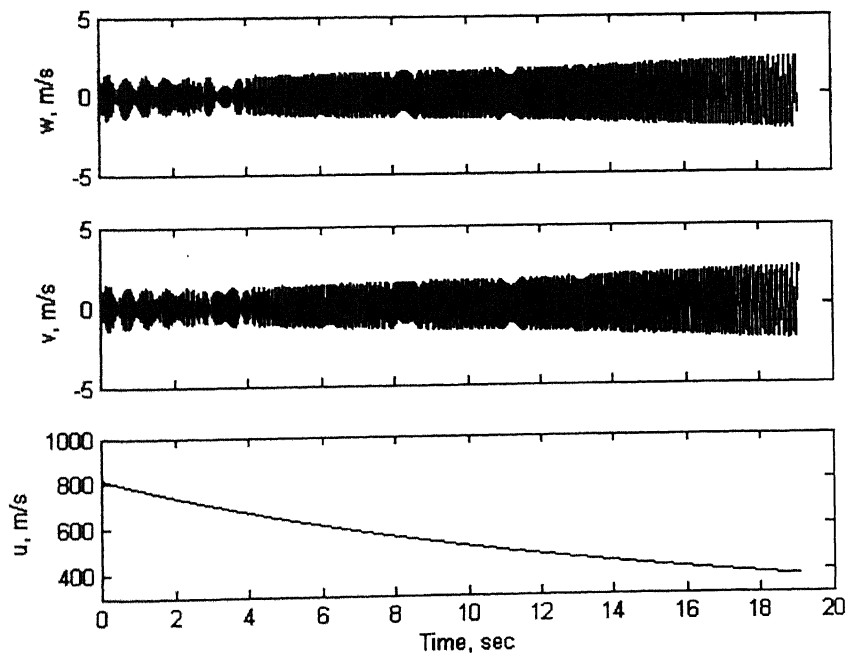


**Fig. 2.9b Typical measured data of u, v, w without noise.**

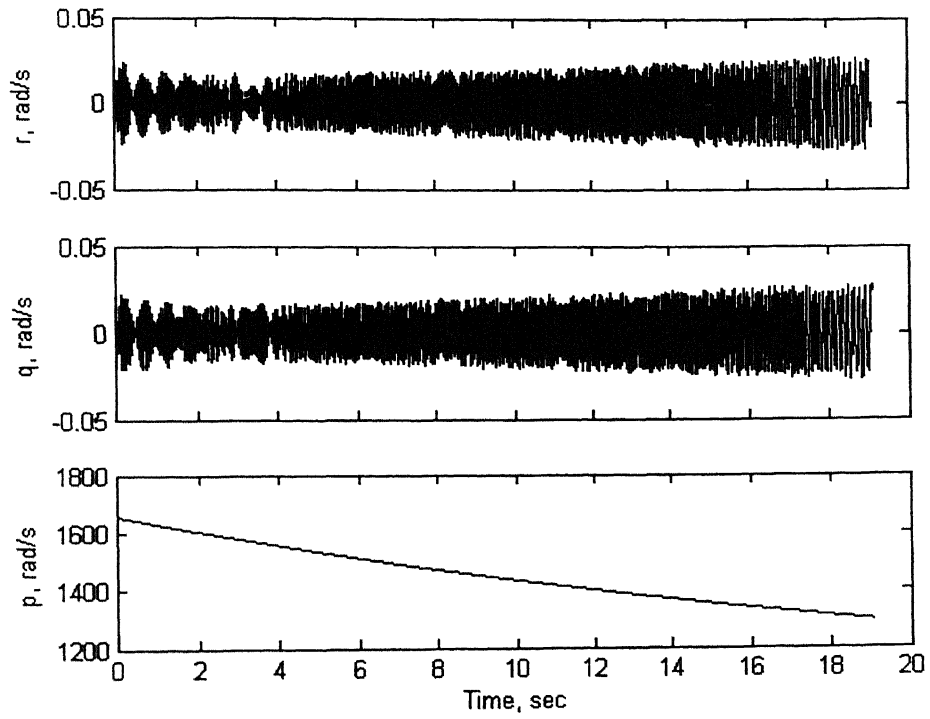


**Fig. 2.9c Typical measured data of  $p$ ,  $q$ ,  $r$  without noise.**

## CHAPTER 3

# RESULTS AND DISCUSSIONS

In this chapter, estimated parameters via ML as well as EKF methods are presented. The simulated flight data corresponding to Ballistic target (FD-BT), Aircraft (FD-AC), Strategic Missile (FD-SM) and Artillery Shell (FD-SDF), are used measured flight data. The effect of measurement noise and initial variance on estimated parameters is also studied. The estimated parameters are presented only with its standard deviation to asses the accuracy of the estimates.

### 3.1 Estimation of ballistic coefficient from ballistic target data (FD-BT)

As stated earlier, here the ballistic target was assumed to fall on a straight-line path directly towards a surface based tracking radar. The ballistic coefficient ( $\beta = \frac{W}{S_{ref} C_{D0}}$ ) is estimated using both ML and EKF method. Table 3.1 compares the estimates obtained using both the methods.

**Table 3.1 Comparison of estimates of ballistic coefficient obtained using both ML and EKF.**

| Initial guess value | Measurement Noise variance | Estimated parameter (Ballistic coefficient) using |                         |
|---------------------|----------------------------|---|-------------------------|
|                     |                            | ML  | EKF                     |
| 600                 | 500                        | 500.1330<br>(0.006163)*                           | 498.2207<br>(0.070775)° |
| 600                 | 1000                       | 500.1881<br>(0.006164)                            | 498.1900<br>(0.070576)  |
| 1000                | 500                        | 500.1330<br>(0.006163)                            | 497.7265<br>(0.069323)  |
| 1000                | 1000                       | 500.1881<br>(0.006164)                            | 497.3556<br>(0.068497)  |

\* CR-Rao bound.

° Standard deviation.

During estimation, the initial guess values were varied from 600 to 1000 (lb/ft<sup>2</sup>) and noise variance were also introduced (500 to 1000 ft<sup>2</sup>). It can be well observed that both the methods estimate the value of Ballistic coefficient very close to the actual value of Ballistic coefficient (500 lb/ft<sup>2</sup>) used for generating the simulated data. Further both the estimates have low standard deviation showing higher confidence of the estimates. It is also noted that, for the particular case estimates are not dependent on the value of initial guess values. Further, both the methods show robustness with respect to noise variance.

### 3.2 Aircraft flight data (FD-AC)

Knowledge of aerodynamic parameters is of paramount importance, to develop accurate mathematical model representing longitudinal dynamics (short-period). The aerodynamic parameters needed to develop the aerodynamic model are force derivatives  $C_{L_0}, C_{L_\alpha}, C_{L_q}, C_{L_\delta}$  and moment derivatives  $C_{m_0}, C_{m_\alpha}, C_{m_q}$  and  $C_{m_\delta}$ . Thus, a study was carried out to explore the possibility of extracting the parameters using both ML and EKF method. Researchers have already presented applicability of both these methods to such flight data<sup>8,9</sup>. However, in this study, this case is included to validate the in-house developed code. Further the effect of noise and type of input on the estimates were also studied to check the robustness of the method.

The flight data ( $\alpha, q$ ) FD-AC1 and FD-AC2 (as given in Fig. 2.6 and Fig. 2.7) were used to estimate the aerodynamic parameters by both ML and EKF method for varied degrees of variance and percentage noise (5% and 10% being presented). Table 3.2 presents the numerical values of the estimated parameters with standard deviations.

**Table 3.2 Comparison of aerodynamic parameters of obtained by using ML and EKF method on FD-AC1 and FD-AC2 with 5% measurement noise.**

| Parameters     | True values of parameters | FD-AC1                |                       | FD-AC2                |                       |
|----------------|---------------------------|-----------------------|-----------------------|-----------------------|-----------------------|
|                |                           | EKF                   | MMLE                  | EKF                   | MMLE                  |
| $C_{l_\alpha}$ | 2.6307                    | 2.6324<br>(0.146776)  | 2.6681<br>(0.1317)    | 2.6170<br>(0.090307)  | 2.6239<br>(0.04294)   |
| $C_{l_q}$      | 4.4134                    | 4.2655<br>(1.005723)  | 4.3077<br>(1.214945)  | 4.3591<br>(0.672155)  | 4.2334<br>(0.367366)  |
| $C_{l_\delta}$ | 1.0425                    | 1.0436<br>(0.04696)   | 1.0556<br>(0.075803)  | 1.0367<br>(0.028275)  | 1.0396<br>(0.036135)  |
| $C_{m_\alpha}$ | -1.16                     | -1.1588<br>(0.008557) | -1.1593<br>(0.009838) | -1.1588<br>(0.00569)  | -1.1581<br>(0.002952) |
| $C_{m_q}$      | -1.1228                   | -1.1122<br>(0.069582) | -1.1019<br>(0.079352) | -1.1254<br>(0.042872) | -1.1267<br>(0.024079) |
| $C_{m_\delta}$ | -0.3557                   | -0.3541<br>(0.002741) | -0.3549<br>(0.007003) | -0.3548<br>(0.001829) | -0.3551<br>(0.002652) |
| $C_{l_0}$      | -0.0522                   | -0.0520<br>(0.002203) | -0.0515<br>(0.003092) | -0.0525<br>(0.002039) | -0.0525<br>(0.003094) |
| $C_{m_0}$      | -0.0163                   | -0.0162<br>(0.000134) | -0.0162<br>(0.000478) | -0.0163<br>(0.000125) | -0.0162<br>(0.000479) |

Referring Table 3.2, it can be observed that both ML and EKF successfully estimated all the parameters. It can be seen that consistently, that estimated parameters (both ML and EKF) using 3-2-1-1 input yields lower values of standard deviation suggesting more confidence in these estimates. Similar observations could be extended for estimated parameters obtained processing flight data with higher degree of noise (10%) as presented in Table 3.3.

**Table 3.3 Comparison of aerodynamic parameters obtained by using ML and EKF method on FD-AC1 and FD-AC2 with 10% measurement noise.**

| Parameters     | True values of parameters | FD-AC1                |                       | FD-AC2                |                       |
|----------------|---------------------------|-----------------------|-----------------------|-----------------------|-----------------------|
|                |                           | EKF                   | MMLE                  | EKF                   | MMLE                  |
| $C_{l_\alpha}$ | 2.6307                    | 2.5248<br>(0.284995)  | 2.7294<br>(0.132548)  | 2.6771<br>(0.179135)  | 2.6546<br>(0.04305)   |
| $C_{l_q}$      | 4.4134                    | 4.6236<br>(1.787376)  | 4.4987<br>(1.227096)  | 3.8604<br>(1.274208)  | 3.4836<br>(0.370112)  |
| $C_{l_\delta}$ | 1.0425                    | 1.0331<br>(0.091799)  | 1.0774<br>(0.075854)  | 1.0644<br>(0.056584)  | 1.0462<br>(0.036349)  |
| $C_{m_\alpha}$ | -1.16                     | -1.1613<br>(0.015394) | -1.1584<br>(0.009927) | -1.1548<br>(0.010797) | -1.1529<br>(0.002944) |
| $C_{m_q}$      | -1.1228                   | -1.1719<br>(0.135488) | -1.0874<br>(0.080165) | -1.1049<br>(0.085014) | -1.1138<br>(0.024137) |
| $C_{m_\delta}$ | -0.3557                   | -0.3567<br>(0.005102) | -0.3545<br>(0.007017) | -0.3553<br>(0.003588) | -0.3552<br>(0.002653) |
| $C_{l_0}$      | -0.0522                   | -0.0525<br>(0.004255) | -0.0501<br>(0.003089) | -0.0527<br>(0.004049) | -0.0534<br>(0.003111) |
| $C_{m_0}$      | -0.0163                   | -0.0163<br>(0.00025)  | -0.0162<br>(0.000477) | -0.0163<br>(0.000245) | -0.0162<br>(0.000477) |

The convergence of the estimated parameters and variance with EKF is pictorially presented in Fig. 3.1 and 3.2. It can be seen that after around 2-5 sec, the error variance converges to zero suggesting accurate estimates.

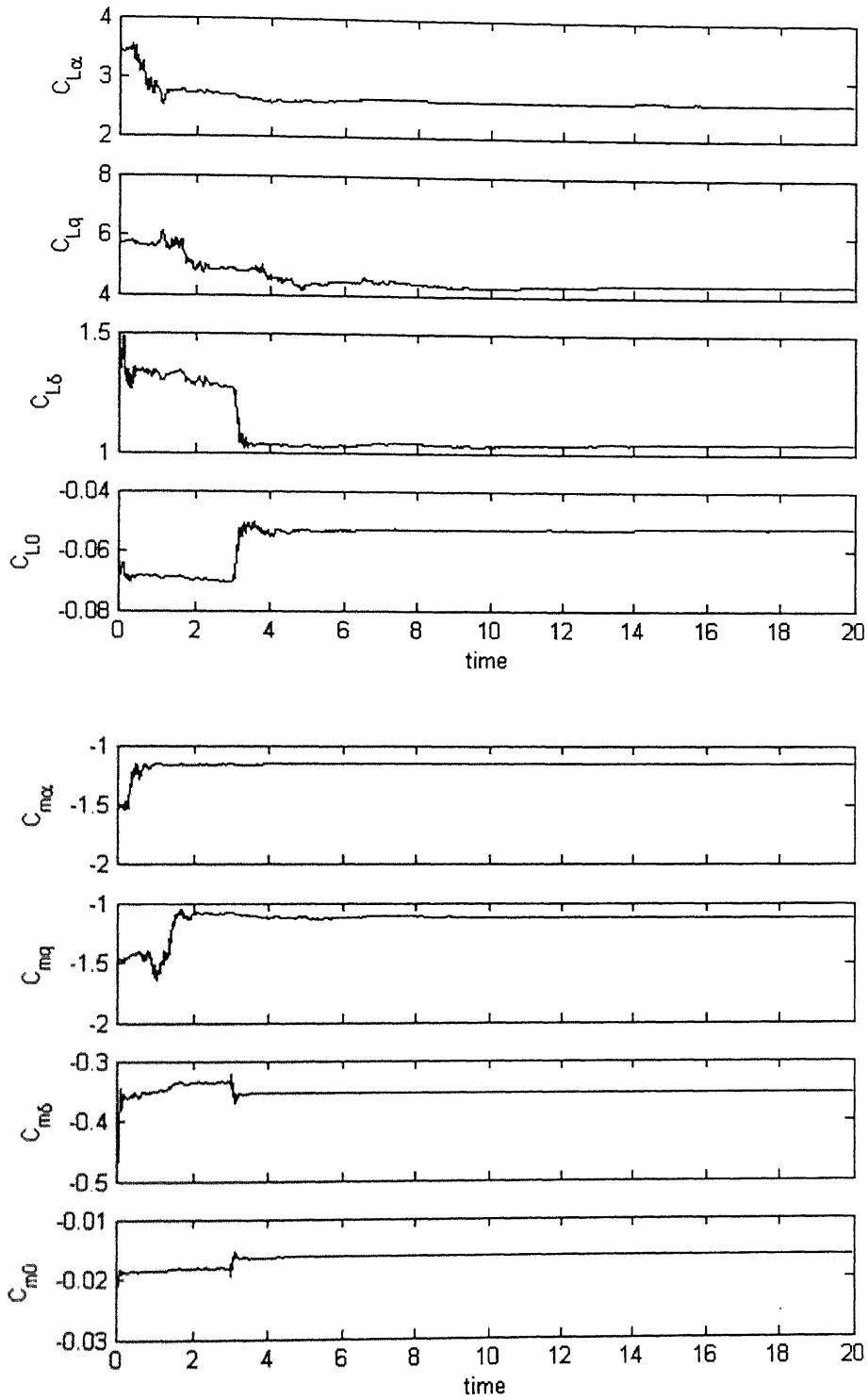


**Fig. 3.1 Convergence of estimated parameters with time for 3-2-1-1 input and 5% measurement noise.**



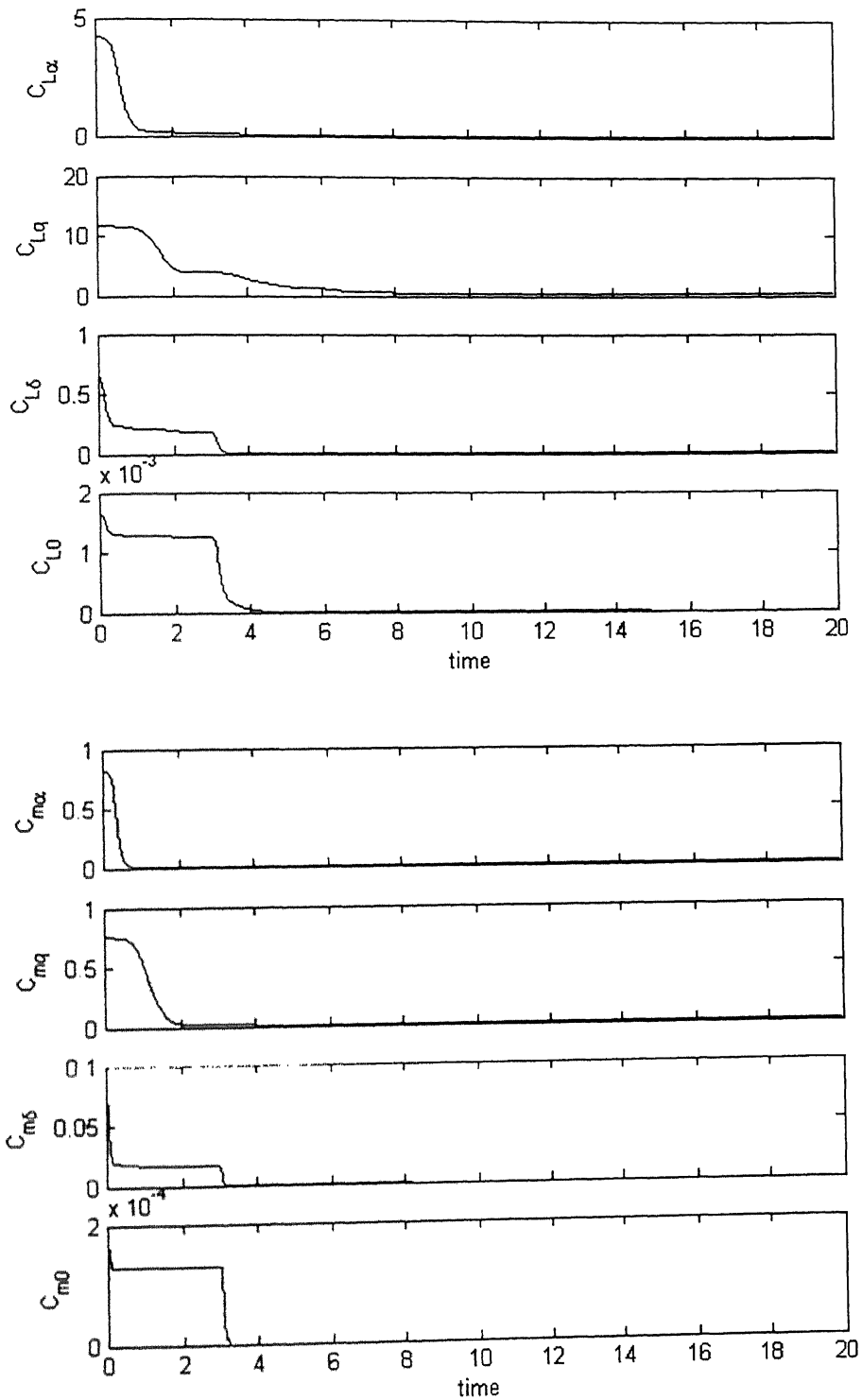


**Fig. 3.2 Convergence of variance with time for 3-2-1-1 input and 5% measurement noise.**

### 3.3 Estimation using flight data of a typical short range strategic missile

The estimation of aerodynamic parameters from flight data of such a missile is more involved as compared to that of an aircraft. It is not always possible to excite the missile with a best input (3-2-1-1). Further due to limitation of having large number of sensors for data acquisition (dedicated for parameter estimation), there is an inadvertent compromise on the quality and quantity of information content in such flight data. It is therefore, important to identify the minimum number of parameters required to be measured to initiate parameter estimation. Due to lack of information content, many a times the estimated parameters tend to become sensitive to the initial guess values. Thus a systematic study was carried out to identify the most suitable combinations of minimum numbers of motion/control variables required for parameter estimation. Various combinations of  $X$ ,  $Y$ ,  $Z$ ,  $q$ ,  $\alpha$ ,  $a_x$  and  $a_z$  were selected and parameters were estimated using various values of initial guess values as presented in Table 3.4. Based on this table, it was decided to have  $X$ ,  $Z$  and  $a_z$  as motion variables to be used for estimation using ML method. Such exercise was also carried out for EKF method and decided to have  $X$ ,  $Z$  and  $q$  as the most appropriate variables for this purpose. It was further observed that the effect of pitch rate ( $q$ ) on  $X$  and  $Z$  were too insignificant. Thus the estimation of  $C_{m_q}$  from these sets of data was not carried out. Such a study using simulated data would be useful in designing the experiment for acquiring the relevant parameters for parameter estimation. However, it may be stressed that such observations must be validated using real flight data. For estimation purpose, ML method used flight data ( $X$ ,  $Z$ ,  $a_z$ ) as presented in Fig. 2.8. Estimated values of aerodynamic parameters with standard deviation are presented in Table 3.5. For both cases of noise level (5% and 10%), ML

method yields lower values of standard deviation as compared to EKF. A study was also carried out to see the effect of initial guess values on the estimated aerodynamic parameters. Typical sets of initial guess values (as presented in Table 3.5) for aerodynamic parameters were chosen. It was found that ML method failed to estimate parameters for the initial guess values-2. However EKF could estimate even with such a deviation in initial guess values. Thus it is observed that for data with limited information, EKF may be used advantageously.

**Table 3.4 Range of initial values for which ML method was able to estimate aerodynamic parameters of a Short range strategic missile.**

| <b>Combination of variables</b> | <b>Range of initial values expressed in percentage.</b> |
|---------------------------------|---|
| $X, Z$                          | -12,12  |
| $X, Z, q$                       | -15,12  |
| $X, Z, a_x$                     | -15,18  |
| $X, Z, a_z$                     | -31,37  |
| $X, Z, \alpha$                  | -12,13  |
| $a_x, a_z, \alpha$              | -10,13  |
| $a_x, a_z, q$                   | -12,10  |
| $a_x, \alpha, q$                | -13,13  |
| $a_z, \alpha, q$                | -10,10  |
| $a_x, a_z, \alpha, q$           | -10,13  |
| $X, Z, a_x, a_z$                | -21,38  |
| $X, Z, a_x, a_z, \alpha$        | -21,38  |
| $X, Z, a_x, a_z, q$             | -21,38  |
| $X, Z, a_x, q, \alpha$          | -11,19  |

**Table 3.5 Comparison of estimated parameters (SM) obtained using ML and EKF method for different initial guess values and measurement noise of 5%.**

| Parameters     | True value | Initial guess values-1 |                       | Initial guess values-2 |                       |
|----------------|------------|------------------------|-----------------------|------------------------|-----------------------|
|                |            | MMLE                   | EKF                   | MMLE                   | EKF                   |
| $C_d$          | 0.3        | 0.3000<br>(5.00E-10)   | 0.2999<br>(1.85E-05)  | Could not estimate     | 0.29984<br>(4.93E-05) |
| $C_{L_\alpha}$ | 5          | 4.9968<br>(4.81E-05)   | 5.0321<br>(0.024639)  |                        | 5.0587<br>(0.068510)  |
| $C_{L_\delta}$ | 2.35       | 2.3459<br>(1.05E-04)   | 2.3967<br>(0.034804)  |                        | 2.4839<br>(0.096597)  |
| $C_{m_\alpha}$ | -6.5       | -6.4998<br>(9.30E-08)  | -6.5012<br>(0.001081) |                        | -6.5042<br>(0.003042) |
| $C_{m_\delta}$ | -8.9       | -8.9000<br>(3.56E-06)  | -8.9064<br>(0.006757) |                        | -8.9660<br>(0.010062) |

Parameters     $C_d$     $C_{L_\alpha}$     $C_{L_\delta}$     $C_{m_\alpha}$     $C_{m_\delta}$

Initial guess values of parameters 1 - 0.2,   3,   3,   -5,   -7

Initial guess values of parameters 2 - 0.2,   2,   4,   -3,   -4

### 3.4 Estimation of aerodynamic parameters using flight data of a typical artillery shell

Due to the non-availability of radar tracked data, simulated flight data were generated using SDF model. Trajectories were generated corresponding to different launch angles. During estimation, the algorithm included PMM, MPMM and SDF progressively. Point mass model can be used advantageously to estimate drag coefficient ( $C_d$ ); however to estimate other derivatives ( $C_d, C_{L\alpha}, C_{m\alpha}, C_{lp}$ ), the estimation algorithm should include higher order of trajectory models, namely MPM or SDF model<sup>20</sup>. The effects of process and measurement noise in the estimation of aerodynamic parameters using EKF method has been presented in detail and are explained case by case.

#### 3.4.1 Estimation using Point Mass Model:

##### Case 1:

During simulation, the drag coefficient along with other parameters was kept as fixed numbers. Their variation with Mach number was not modeled in simulating the trajectory using SDF model. Constant values of aerodynamic parameters used are given in Table 3.6.

**Table 3.6 Values of aerodynamic parameters used for simulation in case 1**

| $C_D$ | $C_{L\alpha}$ | $C_{m\alpha}$ | $C_{lp}$ |
|-------|---------------|---------------|----------|
| 0.3   | 2.0           | 3.0           | -0.025   |

It may be noted that constant approximation for aerodynamic parameters are justified for subsonic flight regime. The estimation algorithm used only Point mass Model and hence expected to estimate the drag coefficient,  $C_d$ . Range (X) and height (Y) corresponding to launch velocity of 818 m/sec and elevation of 7.6 degrees were used as measured

variables. During the implementation of EKF method, numerical differentiation was not used to linearize the state equations; instead the linearized matrix was computed using differentiated terms obtained analytically. For the computation of state transition matrix, first three terms were found to be sufficient. Initially the algorithm was run with measurement noise corresponding to 20m randomly distributed over the whole range without any process noise (assuming the model to be perfect). The estimation process converged to yield a value of 0.28858 for  $C_d$  and convergence of  $C_d$  is graphically presented in Fig. 3.3.

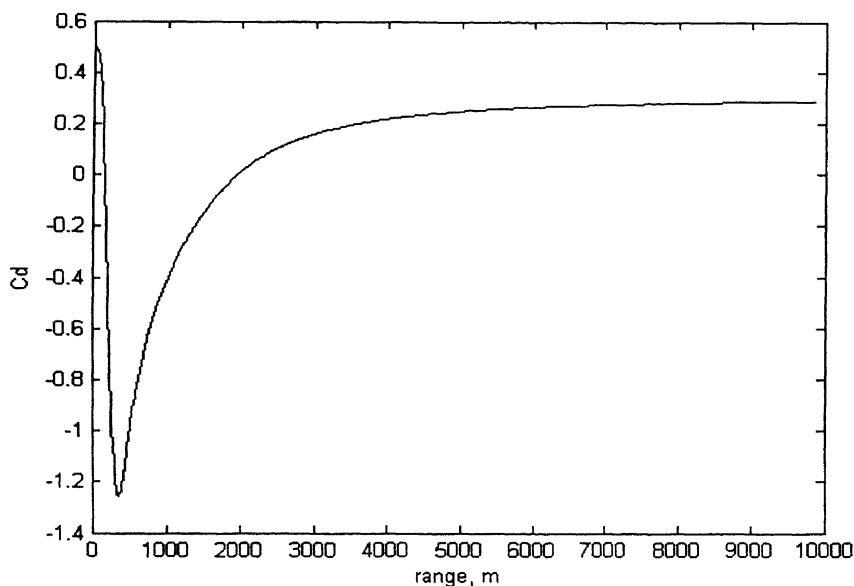


**Fig. 3.3 Convergence of  $C_d$  as plotted w.r.t. range , case1.**

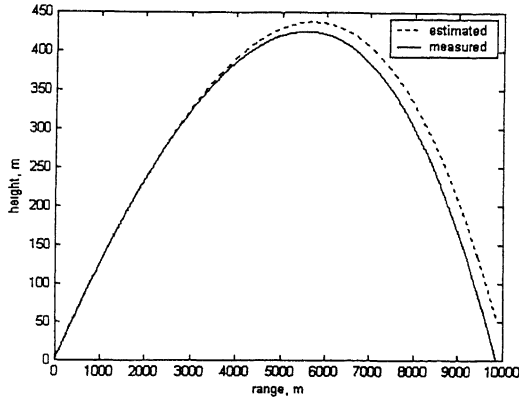


**Fig. 3.4a Comparison of measured and EKF predicted trajectories case1.**

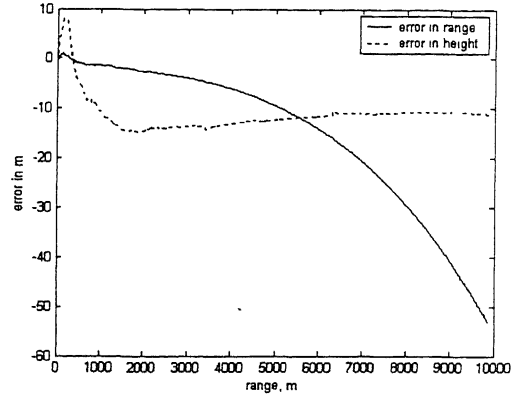


**Fig. 3.4b Error in range and height for case1.**

The estimated trajectory obtained during EKF run is compared with the measured trajectory as shown in Fig. 3.4a. Further, the growth of error in range and height is presented in Fig. 3.4b. It can be observed that, the maximum error in range is about 50m where as in the height about 10m. The estimated value of  $C_d$  is 0.28858 instead of 0.3. In order to improve trajectory matching and the value of estimated  $C_d$ , pseudo-process noise with variance 0.05 and 0.5 were added to X and Z respectively and estimation algorithm was re-run. It was interesting to observe that the matching between measured and estimated trajectories improved considerably, however the estimated  $C_d$  value deteriorated significantly. The convergence of  $C_d$ , error in range and error in height as presented with respect to range presented in Fig. 3.5, 3.6 respectively. It can be observed that the maximum error has come down to 10m in range and 2m in height. However, it can be seen from Fig. 3.5, that the  $C_d$  value converged to 0.2369, instead of actual value of 0.3 showing further deterioration.

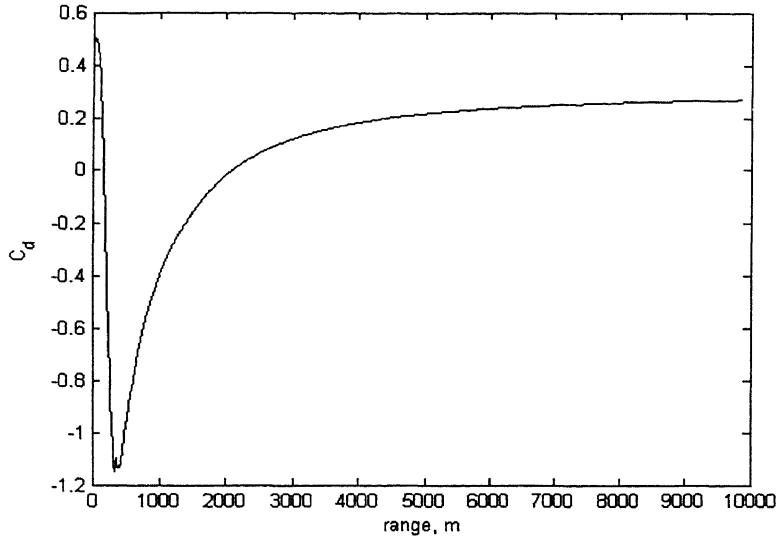


**Fig. 3.5 Convergence of  $C_d$  as plotted w.r.t. range**

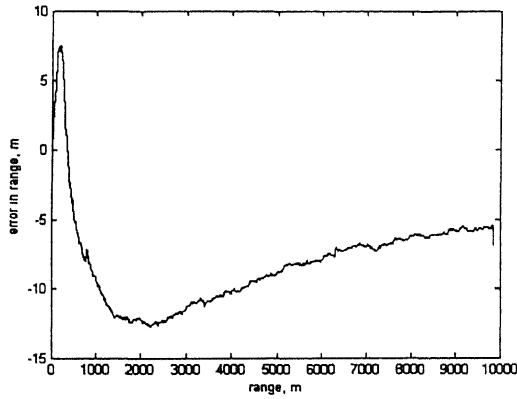


**Fig. 3.6a Comparison of measured and EKF predicted trajectories.**

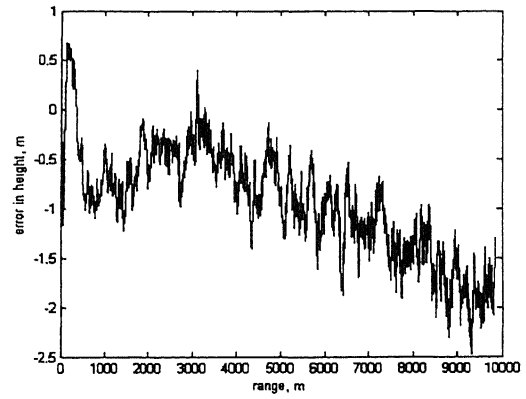


**Fig. 3.6b Error in range and height**

In order to improve  $C_d$  value, a pseudo-noise of  $1 \times 10^{-7}$  was also added to  $C_d$  and the flight data X and Z were processed to estimate the drag coefficient  $C_d$ . In this run, process noise for X and Z were kept fixed at 0.01 and 0.1 respectively. The estimated value of  $C_d$  showed remarkable improvement by converging to actual value of  $C_d$  used for simulation. This improved convergence is presented pictorially in Fig. 3.7. Further it was observed that the maximum error in range and height remained well within 10m and 2m respectively.



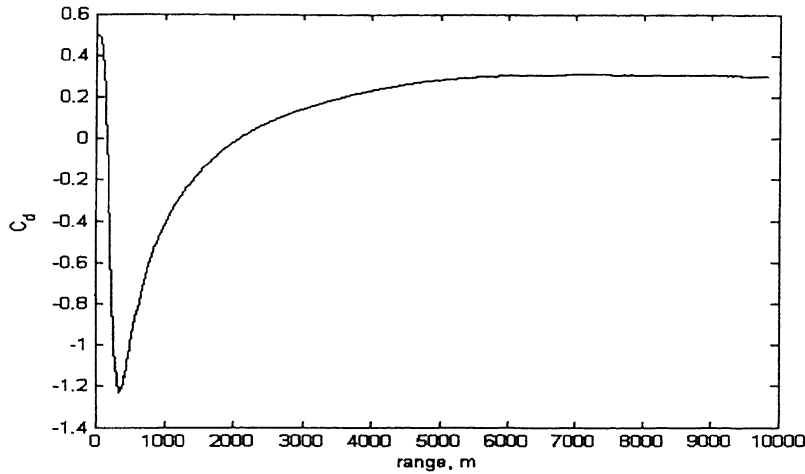


**Fig. 3.7 Convergence of Cd**

**Case 2: Estimation of  $C_d$  V/s Mach number using Point Mass Model:**

The artillery shells when fired are expected to travel Mach number covering subsonic to supersonic regime. The aerodynamic parameters are strong functions of mach numbers. Therefore, it is important to extract aerodynamic parameters as a function of Mach number. In this case EKF was applied using the PMM to estimate functional dependence of  $C_d$ . The simulated data were generated by using aerodynamic parameters (as function of Mach number) given in Table 2.7. Process noise was added to X, Z and  $C_d$  (0.01, 0.1, 0.0001) respectively. EKF routine was run to obtain estimated value of range, height and  $C_d$  as function of Mach number as presented in Fig. 3.8 and 3.9 respectively.

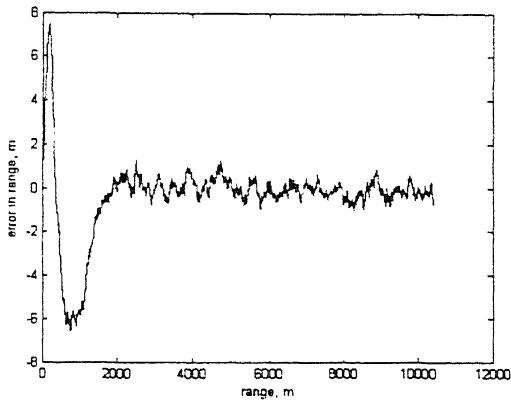


**Fig. 3.8a Error in range.**

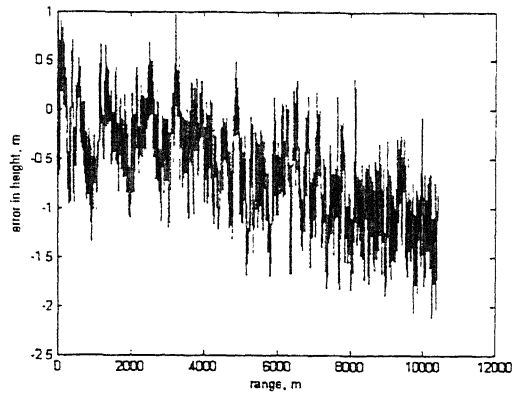


**Fig. 3.8b Error in height.**

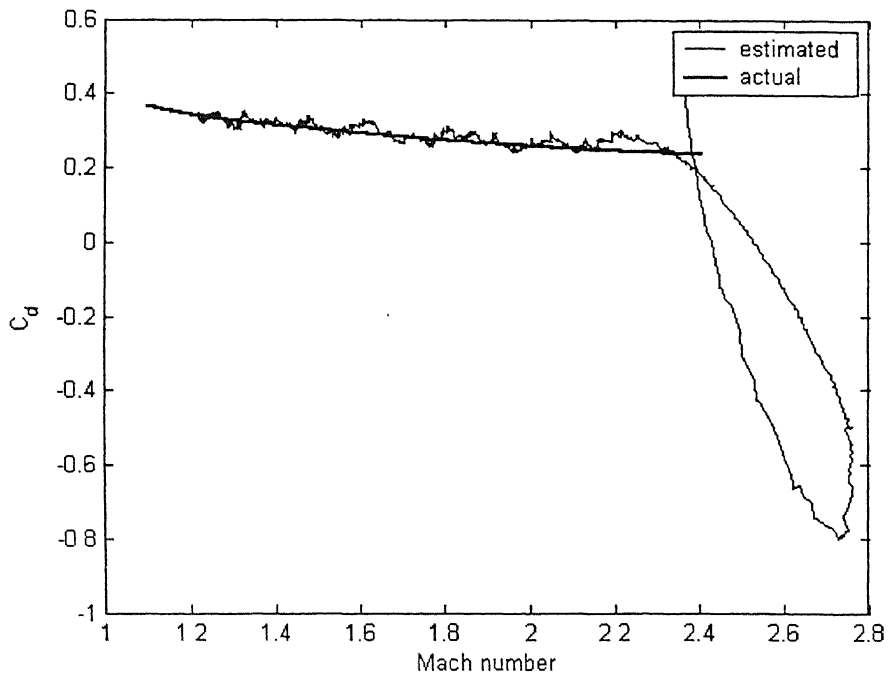


**Fig. 3.9  $C_d$  Vs Mach number for case2, FD-SDF**

Referring Fig. 3.8(a) and (b), it can be seen that the estimated max error in range and height are well within 7m and 1.5m respectively. The estimated value of  $C_d$  as function of Mach number presented in Fig. 3.9 compares well with the manufacturer supplied value of  $C_d$  Vs Mach number. Thus, it can be concluded that EKF can be advantageously applied to extract functional dependence of drag coefficient on Mach number. Similar

observations, related to application of ML method to the above mentioned cases have been reported in ref (20).

### **3.4.2 Estimation of aerodynamic parameters using MPM:**

Due to non-availability of measured flight data, simulated flight data (FD-SDF) were first constructed using constant aerodynamic parameters and then using aerodynamic parameters as function of Mach number. However, in the estimation algorithm MPM model was used for this case.

#### **3.4.2.1 Flight data simulated with constant aerodynamic parameters:**

Aim of this study was to investigate the capability of EKF method in extracting constant aerodynamic parameters using measured trajectory coordinates X, Y and Z. Successful implementation of ML method (  $C_d, C_{L\alpha}, C_{m\alpha}, C_{lp}$  ), in extracting the above parameters are reported in Ref 20. However during estimation  $C_{L\alpha}$  has been kept fixed to its true value. The EKF method was implemented and was successful only in estimating the parameters  $C_d, C_{lp}$  correctly. However the parameters  $C_{L\alpha}$  and  $C_{m\alpha}$  showed poor convergence. In order to improve their estimates, initial value for  $C_{m\alpha}$  was set at the exact value, and it was seen as presented in Fig. 3.10. that the convergence of  $C_{L\alpha}$  improves remarkably.

#### **3.4.2.2 Flight data simulated using aerodynamic parameters varying with Mach number.**

The concept of using aerodynamic parameters as constant values is strictly valid for low subsonic flight. However the shells under investigation are supposed to cover flight regime covering subsonic to supersonic flow. Thus it is important to capture the Mach number dependence of these parameters in developing accurate mathematical

model. During implementation of EKF method, it was observed that it was not possible to extract all these parameters simultaneously using only X, Y and Z. Several trials were attempted to arrive at a particular combination of motion variables, which could be used

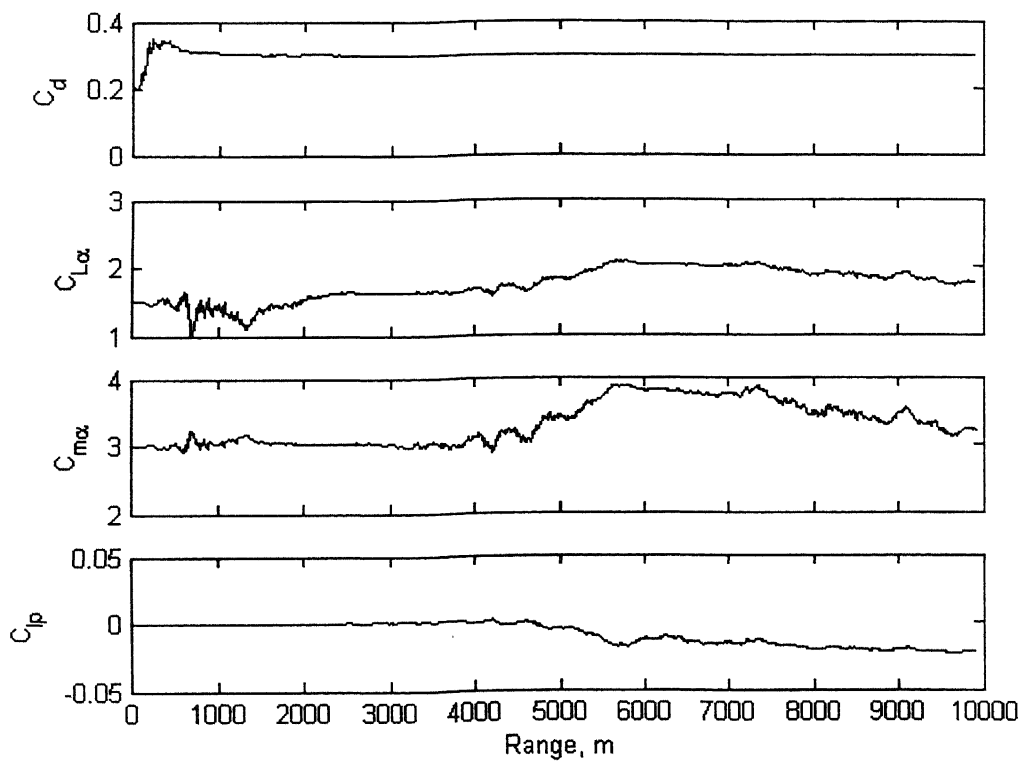


**Fig. 3.10 Estimation of constant parameters using MPM from FD-SDF.**

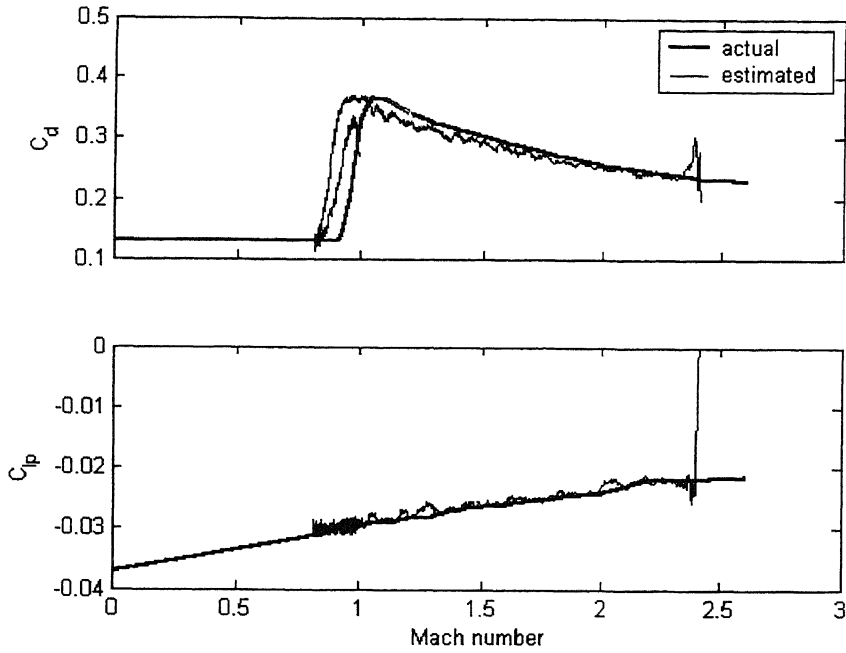


**Fig. 3.11 Estimation of  $C_d$  and  $C_{lp}$  as a function of Mach number (45 degrees elevation).**

to estimate only few aerodynamic parameters as function of Mach number. The flight data used for this purpose included  $X$ ,  $Y$ ,  $Z$ ,  $u$ ,  $v$ ,  $w$  and  $p$ . The implementation of EKF resulted in estimation of  $C_d$  and  $C_{lp}$  as function of Mach number, the comparison of  $C_d$  and  $C_{lp}$  estimated through EKF and actual are presented in Fig 3.11. However the mach number dependence of  $C_{L\alpha}$  and  $C_{m\alpha}$  could not be captured with this flight data. One possible reason could be due to the fact that the trajectory angle of attack of shells is well within 0-0.3 degree for most of the flight path. Thus, the effect of  $C_{L\alpha}$  and  $C_{m\alpha}$  on range and deviations are too small to be sensitive for their estimation. There is a need to carryout detail study to modify the strategy to capture these variations. For the sake of completion, it may be mentioned that similar observations were noted while implementing EKF using SDF model.

During the estimation process, it was observed that ML methods are highly sensitive to the correctness of initial values of motion variables, however, EKF can advantageously applied by appropriately modifying process noise to handle such inherent error present in acquiring trajectory data. This is perhaps a unique advantage, with EKF which designers utilized rigorously for implementation of on-line control law and guidance schemes.

## CHAPTER 4

# CONCLUSIONS AND SUGGESTIONS FOR FUTURE WORK

### 4.1 Conclusions

In the present work, ML and EKF methods have been applied to estimate aerodynamic parameters from simulated radar tracked data. These methods have been applied starting from a one-dimensional Ballistic target to an artillery shell, longitudinal motion of strategic missile and also to flight data of an aircraft. It is observed that both EKF and ML methods can be applied successfully to estimate all the parameters from flight data of an aircraft. However for shells/rockets, both the methods are capable of estimating only drag coefficient,  $C_d$  and roll damping coefficient  $C_{lp}$  accurately. Both the methods failed to estimate the aerodynamic parameters  $C_{L\alpha}$  and  $C_{m\alpha}$ . However, for SM, it was found that, if appropriate flight data is generated, both the methods can be used advantageously to estimate force and moment derivatives.

### 4.2 Suggestions for future work

1. In the present work, simulated flight data were used to estimate aerodynamic parameters of the artillery shell and strategic missile due to non-availability of the real flight data. The capability of these methods should however be validated using real flight data.
2. Scope of EKF may be expanded to capture Mach number dependence of all the parameters.

3. The simulated data was generated for standard atmospheric conditions. Applicability of these methods to estimate parameters using flight data under non-standard atmospheric conditions may be explored.
4. Filter error method which uses Kalman Filter for state estimation and ML method for parameter estimation could also be explored.

गुरुशोभम काशीनाथ केसकर पुस्तकालय  
भारतीय प्रौद्योगिकी संस्थान कानपुर  
अवधि क्र० A-148451



## REFERENCES

1. Anonymous, "Text Book of Ballistics and Gunnery (TBBG)", Vol.2, HMSO, London, 1987.
2. Seckel, E. and Morris, J.J., "The Stability Derivatives of the Navion Aircraft Estimated by Various Methods and Derived from Flight Test Data", FAA-RD-71-6.
3. Seckel, E., "Stability and Control of Airplanes and Helicopters", Academic Press, New York, 1964.
4. Ellison, D.E., USAF: "Stability and Control Handbook (DATCOM)", Wright Patherson Air Force Base, Ohio, Revised August 1968.
5. Maine, R.E. and Iliff, K.W., "Identification of Dynamic System-theory and Formulations", NASA RP 1138, Feb 1985.
6. Pietrass, A. "Determination of Aerodynamic Derivatives of the F1A1A G9 IT3 Aircraft from Flight Test by means of Manual Analog Model Matching", Paper No. N75-19257 of Publication ESRO TT-104, Nov 1974.
7. Taylor, L. W., Iliff, K.W. and Powers, B.G. "A comparison of Newton-Raphson and other methods for Determining Stability Derivatives from Flight Data", AIAA Paper No. 69-315, May 1969.
8. Peter G. Hamel, Jategaonkar, R.V., "The evolution of Flight Vehicle System Identification" AGARD, DLR, Germany, 8-10, May 1995.
9. Jategaonkar, R.V., Plaetschke, E., "Algorithms for Aircraft Parameter Estimation Accounting for Process and Measurement Noise", Journal of Aircraft, Vol.26, No.4,1989,pp.360-372.
10. Kalman, R.E., "A New Approach to Linear Filtering and Prediction Problems", Transactions of the American Society of Mechanical Engineers, Series D, Journal of Basic Engineering, Vol. 82, March 1960, pp.35-45.
11. Maybeck, P.S., "Stochastic Models, Estimation, and Control", Vol.1, Academic Press, 1979.

12. Grewal, M.S., Andrews, A.S., "Kalman Filtering-Theory and Practice Using MATLAB", Second Edition, John Wiley & Sons, 2001.
13. Mehra, R., "On the identification of variances and Adaptive Kalman filtering", IEEE transactions on Automatic Control, Vol. AC-15, No.2, 1970, pp.175-184.
14. Morelli, E., "Estimating noise Characteristics from Flight Test Data Using Fourier Smoothing", AIAA Paper 94-0152, Jan. 1994.
15. Myers, K.A., Tapley, B.D., "Adaptive sequential estimation with Unknown Noise Statistics", IEEE Transactions on Automatic Control, Vol. Ac 21, 1976, pp 520-525.
16. Winchenbach, G.L., Randy S. Buff, white, R. H. and Hathaway, W.H. "Subsonic and Transonic Aerodynamics of a Wrap around Fin Configuration", Journal of Guidance, Vol.9, No.6, Nov-Dec 1986.
17. Dupis Alan D., "High spin effect on the Dynamics of a high l/d Finned Projectile from Free-Flight Tests", Journal of Guidance, Vol.12, No.2, March-April 1989, pp.129-134.
18. Zarchan, "Tactical and Strategic Missile Guidance and Control", AIAA,1997.
19. Nelson, "Flight stability and automatic control", Second Edition, Mc-Graw Hill,1997.
20. Sridhar,I.V.S., "Parameter estimation from radar tracked flight data of an artillery shell", M.Tech. Theses, Department of Aerospace Engineering, IIT Kanpur, December 2002.

## APPENDIX A

### EXTENDED KALMAN FILTER

Kalman filter applied to non-linear systems is known as EKF. Parameter estimation is inherently a non-linear problem whether the system is linear or non-linear.

The dynamic system, whose parameters are to be estimated, is assumed to be described by the following stochastic equations.

$$\begin{aligned}\dot{x}(t) &= f[x(t), u(t)] + w(t) & x(t_0) &= x_0 \\ z(k) &= h[x(k), u(k)] + v(k) & k &= 1, \dots, N\end{aligned}$$

First equation represents the system dynamics and the second the measurement dynamics. The  $n$  and  $m$  dimensional system functions  $f$  and  $h$  are general nonlinear real valued vector functions. These system functions are assumed to have sufficient differentiability to be able to invoke Taylor series expansion. The  $m$ -dimensional measurement  $z$  is sampled at  $n$  discrete time points with a uniform sampling time  $\Delta t$ .

It is assumed that the process and measurement noise  $w$  and  $v$  affect the dynamic system linearly. They are assumed to be characterized by a zero-mean white Gaussian noise with covariances of  $Q$  and  $R$  respectively.

The above dynamic model is for state estimation. For parameter estimation the unknown parameters  $\theta$  are added as additional state variables considering them as the output of an auxiliary dynamic system

$$\dot{\theta} = 0$$

The augmented state vector  $X$  is defined as  $X^T = \{x^T, \theta^T\}$ .

Now the extended system can be represented as

$$\begin{aligned}\dot{X}(t) &= f_a[X(t), u(t)] + w_a(t) \\ &= \begin{bmatrix} f[x(t), u(t)] \\ 0 \end{bmatrix} + \begin{bmatrix} w(t) \\ 0 \end{bmatrix}\end{aligned}$$

$$z(k) = h_a[X(k), u(k)] + v(k)$$

where the subscript a denotes augmented system vectors.

### EKF algorithm:

The initial conditions  $X(0)$ ,  $P(0)$  and the noise covariance matrices  $Q$  and  $R$  need to be known before applying the algorithm. In the present theses process noise is assumed to be zero and the simulated data is generated with constant measurement noise  $R$ .

Step 1: Time update (effect of dynamics)

$$\begin{aligned}X_k^- &= X_k^+ + \int_{t_{k-1}}^{t_k} f[X(t), u(t)] dt \\ P_k^- &= \phi_{(k,k-1)} P_k^+ \phi_{(k,k-1)}^T + Q\end{aligned}$$

Step 2: Measurement update (effect of measurement)

$$\begin{aligned}K_k &= P_k^- H_k^T [H_k P_k^- H_k^T + R]^{-1} \\ P_k^+ &= [I - K_k H_k] P_k^- [I - K_k H_k]^T + K_k R K_k^T \\ X_k^+ &= X_k^- + K_k [z_k - H_k X_k^-]\end{aligned}$$

Superscripts ‘-’ and ‘+’ denote the predicted and corrected state estimates/covariances respectively. Step 1 and step2 are also called as prediction and correction steps in Kalman filter.

The state transition matrix  $\phi_{(k,k-1)}$  is given by  $e^{Ft}$

where F is given by

$$F_k = \left. \frac{\partial f_a[X(k), u(k)]}{\partial X(k)} \right|_{X_k = X_{k-1}^+}$$

$$\text{also } H_k = \left. \frac{\partial h_a[X(k), u(k)]}{\partial X(k)} \right|_{X_k = X_k^-}$$

$X^-$  is the predicted state vector from integration over the time step of measurement data

$X^+$  corrected state vector using the measurements.

$P^-$  predicted/apriori error covariance matrix. It gives error in the predicted states.

$P^+$  corrected/posteriori error covariance matrix. It gives the error in the corrected estimates.

$R$  the measurement noise covariance, determines how much information from the sample is used

$Q$  the model/input noise covariance contribute to the overall uncertainty of the estimate as it is added to  $P^-$  in each time step.

$K$  the Kalman gain determines how much of the innovation (the difference between the actual measurement and model measurements) is used to correct the estimate.

## APPENDIX B

# MAXIMUM LIKELIHOOD (ML) METHOD

The parameter estimation algorithm used in this study is the conventional ‘Maximum Likelihood Method’. The programs were written in ‘C’ using the MLE algorithm. The algorithm is given as follows:

Let a mathematical model of a system be represented by the following equations:

$$X(t_i) = A X(t_i) + B U(t_i) \quad (\text{A.1})$$

$$Z(t_i) = C X(t_i) + G n_i \quad (\text{A.2})$$

where  $X$  is the state vector,  $U$  the control vector,  $Z$  the measured (observation) response and  $n_i$  is the noise vector respectively. The matrices  $A$  and  $B$  contain the unknown stability and control derivatives (parameters). If there is no state noise and the matrix  $GG$  is known, then the Maximum Likelihood estimator minimizes the cost function,

$$J(\theta) = (1/2) \sum_{i=1}^n \left\{ \left[ Z(t_i) - Z_{\theta}(t_i) \right]^T (GG^T)^{-1} \left[ Z(t_i) - Z_{\theta}(t_i) \right] \right\} \quad (\text{A.3})$$

where  $GG^T$  is the measurement noise covariance matrix and  $Z_{\theta}(t_i)$  is the computed response estimate of  $Z$  at  $t_i$  for a given value of the unknown parameter vector  $\theta$ . The cost function is a function of the difference between the measured and computed time histories. In our case, we have taken  $GG^T = 1$  for the cost function. To minimize the cost

function  $J(\theta)$ , we can apply the Newton-Raphson algorithm, which chooses successive estimates of the vector  $\theta$  of unknown coefficients. If  $k$  is the iteration number, then

$$\theta_{k+1} = \theta_k - \left[ \nabla_{\theta}^2 J(\theta_k) \right]^{-1} \left[ \nabla_{\theta}^T J(\theta_k) \right], \quad (\text{A.4})$$

where the first gradient is defined by

$$\nabla_{\theta} J(\theta) = - \sum_{i=1}^n \left\{ \left[ Z(t_i) - Z_{\theta}(t_i) \right]^T (GG^T)^{-1} \left[ \nabla_{\theta} Z_{\theta}(t_i) \right] \right\}, \quad (\text{A.5})$$

and the second gradient is approximated by

$$\nabla_{\theta}^2 J(\theta) = \sum_{i=1}^n \left\{ \left[ \nabla_{\theta} Z_{\theta}(t_i) \right]^T (GG^T)^{-1} \left[ \nabla_{\theta} Z_{\theta}(t_i) \right] \right\}. \quad (\text{A.6})$$

The matrix  $GG^T$  is approximated by a diagonal matrix, with the diagonal elements given by,

$$\sum_{i=1}^n \frac{\left\{ \left[ Z(t_i) - Z_{\theta}(t_i) \right] \left[ Z(t_i) - Z_{\theta}(t_i) \right]^T \right\}}{N}, \quad (\text{A.7})$$

where  $N$  is total number of data points. The term  $\nabla_{\theta} Z_{\theta}(t_i)$  occurring in the first and the second gradients is evaluated by finite difference approximation for each of the sensitivity coefficients present in it. For example, to evaluate sensitivity coefficient

$\frac{\partial \alpha}{\partial C_{mq}}$ , the equations of motion are solved to obtain  $\alpha$  for  $C_{mq} + \Delta C_{mq}$  and  $C_{mq} - \Delta C_{mq}$ .

Let the respective values of  $\alpha$  be  $\alpha^+$  and  $\alpha^-$ , then we have

$$\frac{\partial \alpha}{\partial C_{mq}} = \frac{\alpha^+ - \alpha^-}{2\Delta C_{mq}}$$

The reliability of the estimated parameter in terms of the Cramer-Rao bounds is given by the square root of the diagonal elements of  $\left[ \nabla_{\theta}^2 J(\theta_k) \right]^{-1}$ , which is anyway evaluated as part of the ML algorithm.

In the present work, for estimating the aerodynamic parameters of the artillery shell, the vector of unknown parameters is given by  $\theta = [C_d, C_{L\alpha}, C_{m\alpha}, C_{lp}]$  for a typical case with the  $Z(t_i)$  and  $Z_{\theta}(t_i)$  responses being computed by the spatial coordinates  $x, y$  and  $z$  respectively.